Seminar
DESY/Zeuthen
Thursday, April. 7, 2011

Laser Acceleration and High Field Science

Toshiki Tajima
LMU and MPQ, Garching

Acknowledgments for Collaboration and advice: G. Mourou, W. Leemans, K. Nakajima, K. Homma, D. Habs, K. Witte, C.. Barty, P. Chomaz, D. Payne, H. Videau, P. Martin, V. Malka, F. Krausz, T. Esirkepov, S. Bulanov, M. Kando, W. Sandner, A. Suzuki, M. Teshima,, B. Cros, J. Chambaret, E. Esarey, R. Assmann, R. Heuer, A. Caldwell, S. Karsch, F. Gruener, M. Zepf, M. Somekh, E. Desurvire, D. Normand, J. Nilsson, W. Chou, F. Takasaki, M. Nozaki, K. Yokoya, D. Payne, S. Chattopadhyay, P. Bolton, E. Esarey, S. Cheshkov, C. Chiu, M. Downer, C. Schroeder, J.P. Koutchouk, K. Ueda, Y. Kato, E. Goulielmakis, X. Q. Yan, J. E. Chen, R. Li, J. Rossbach, A. Ringwald, E. Elsen, U. Husemann, A. Chao, F. Stephan, W. Lohmann

1. Relativity drives coherence:
   Relativistic Optics, Laser Wakefield, FEL
2. Applications of Laser Wakefield Accelerator:
   cancer therapy (IORT), ultrafast radiolysis,
   THz, X-ray radiation sources, compact XFEL,
   ion acceleration, collider, collective decelerator,
   even physics of heavy ion collisions
3. Bridge between laser and accelerator communities:
   ICUIL-ICFA collaboration, Bridgelab,….
4. A future collider option
5. Collider physics challenges
6. Laser technology development for collider: ICAN
7. Energy frontier at PeV with attosceond metrology
8. High Field explores low energy new fields

Energy frontier ← High field science, high intensity laser

relativistic optics: *relativistic coherence*

cf. quantum optics: *quantum coherence*

Quantum optics
Cold Atoms
feV-neV

2010

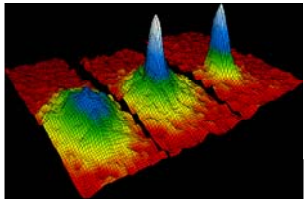

1eV

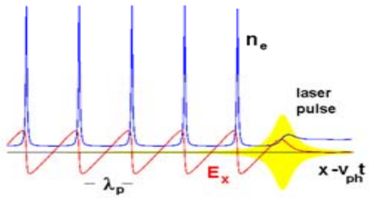

Relativistic
optics
GeV-TeV

2010

1960

Cohen-Tannoudji,Chu,
Ketterle,…

Relativistic Optics, RMP, Mourou (2006)

High field science ⟷ **High energy Physics (fundamental physics)**

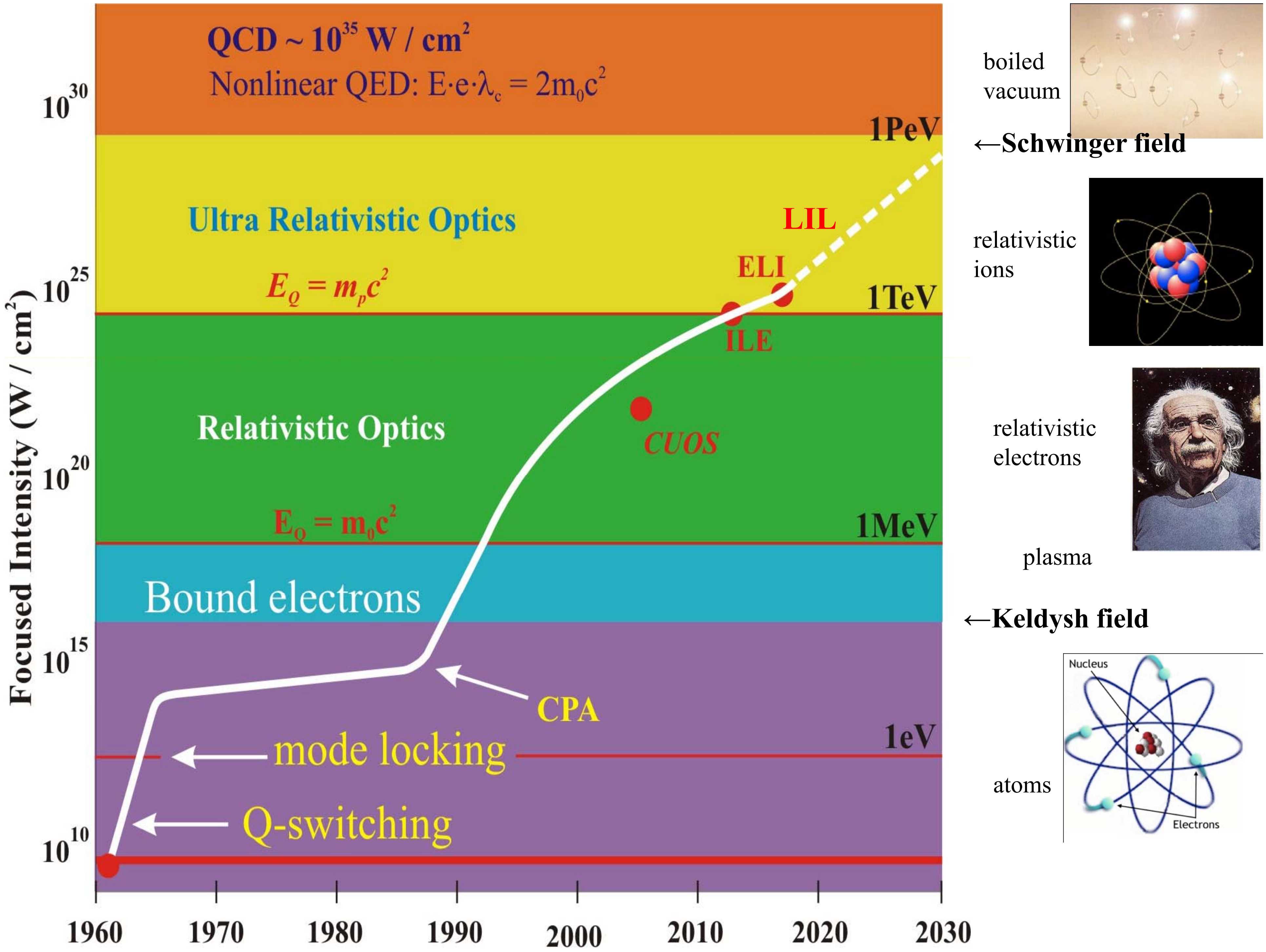

QCD ~ 10^{35} W / cm^2
Nonlinear QED: $E \cdot e \cdot \lambda_c = 2m_0c^2$
Ultra Relativistic Optics
$E_Q = m_pc^2$
Relativistic Optics
$E_Q = m_0c^2$
Bound electrons
mode locking
Q-switching
CPA
LIL
ELI
ILE
CUOS
1PeV
1TeV
1MeV
1eV
Focused Intensity (W / cm^2)
10^{30}
10^{25}
10^{20}
10^{15}
10^{10}
1960
1970
1980
1990
2000
2010
2020
2030
boiled vacuum
←Schwinger field
relativistic ions
relativistic electrons
plasma
←Keldysh field
atoms
Nucleus
Electrons

Relativistic nonlinearity under intense laser

a) Classical optics : $v<<c$,

$a_0<<1$: δx only

b) Relativistic optics: $v\sim c$

$a_0>>1$: $\delta z >> \delta x$

$$a_0 = \frac{eA_0}{mc^2} = \frac{eE_0\lambda}{mc^2}$$

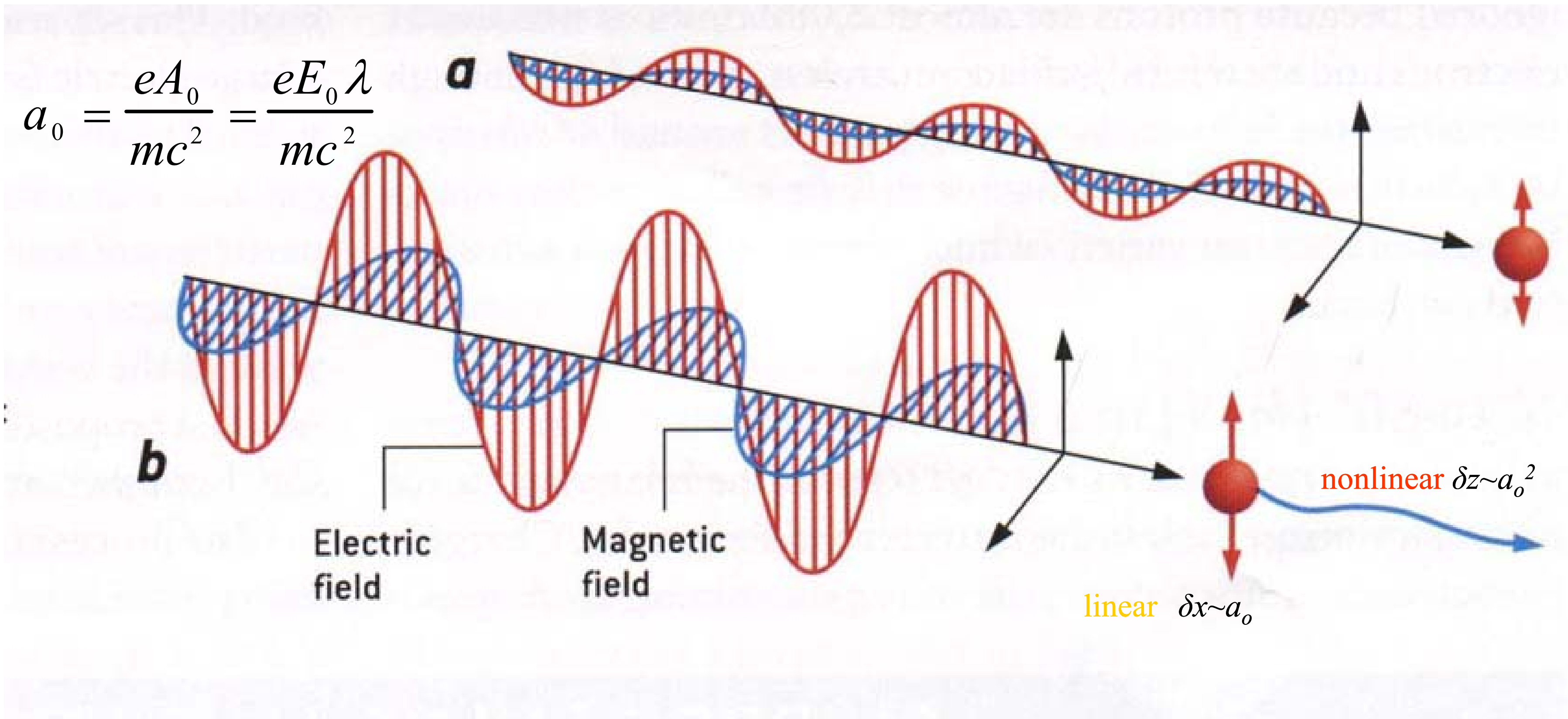

Wakefield : a Collective Phenomenon

All particles in the medium participate = collective phenomenon

Kelvin wake

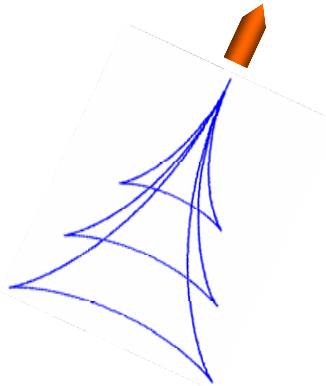

Colletive dynamics

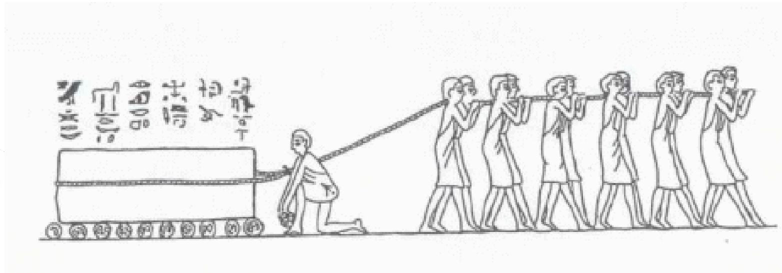

(cf. individual
particle dynamics)

No wave breaks and wake **peaks** at v≈c

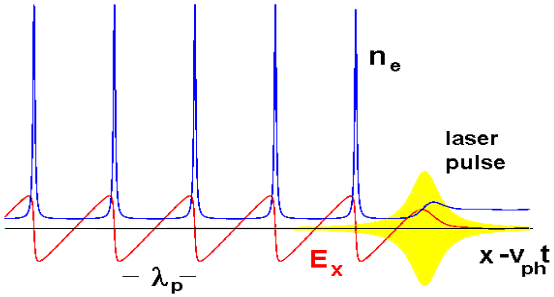

(The density cusps.
Cusp singularity)

← **relativity regularizes**

Wave **breaks** at v<c

Hokusai

Intra-Operative Radiation Therapy (IORT)

LWFA* electron sources: *technology transferred to company

NOVAC7 *(HITESYS SpA)* *RF-based*	vs.	**CEA-Saclay experim. source** *Laser-based*
El. Energy < 10 MeV (3, 5, 7, 9 MeV)		*El. Energy > 10 MeV (10 - 45 MeV)*
Peak curr. 1.5 mA		*Peak curr. > 1.6 KA*
Bunch dur. 4 μs		*Bunch dur. < 1 ps*
Bunch char. 6 nC		*Bunch char. 1.6 nC*
Rep. rate 5 Hz		*Rep. rate 10 Hz*
Mean curr. 30 nA		*Mean curr. 16 nA*
Releas. energy (1 min) @9 MeV (≈dose) 18 J		*Releas. energy (1 min) @20 MeV (≈dose) 21 J*

(A. Giulietti et al., Phys. Rev. Lett.,2008 : INFN)

Table-top Brilliant Undulator X-ray Radiation from LWFA

(M. Fuchs, et al., Nature Phys., 2009)

Observed undulator radiation spectrum

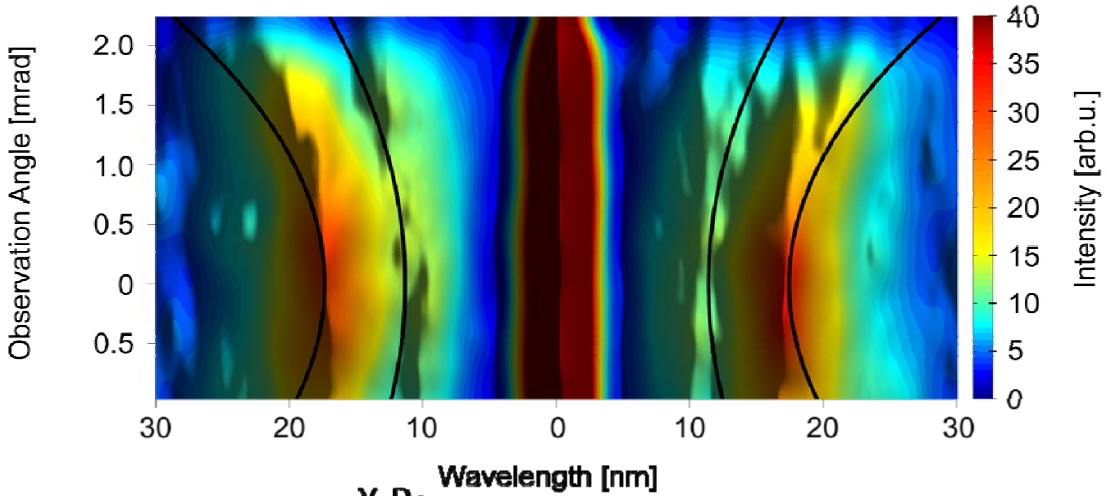

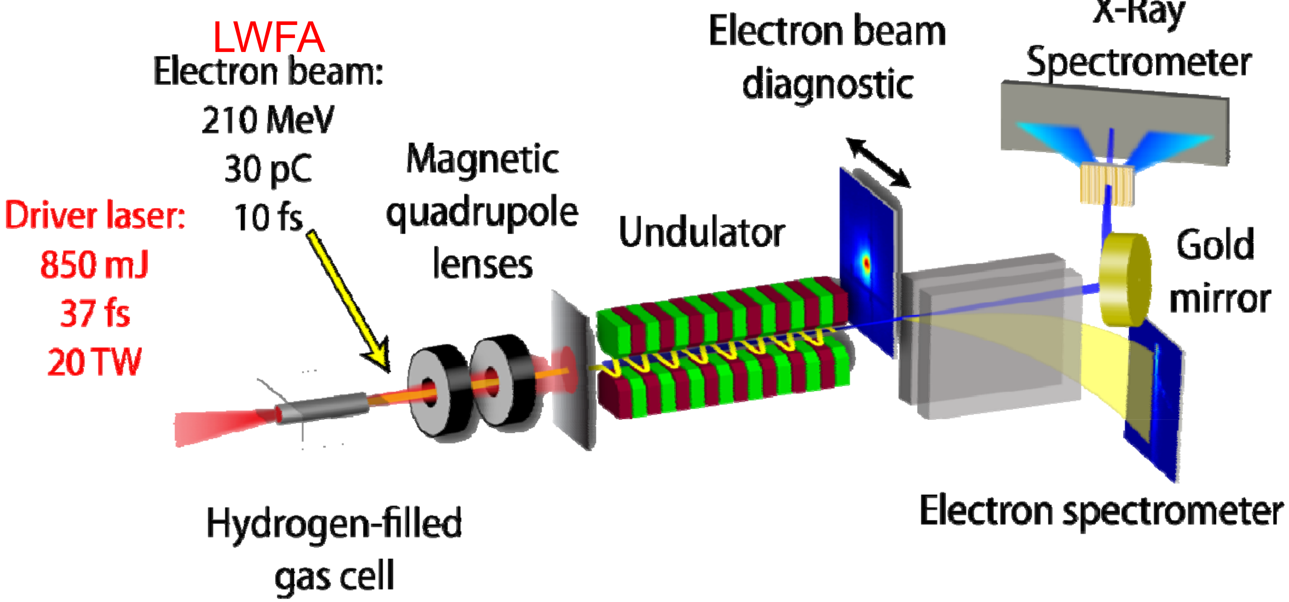

Livingston Chart and Recent Saturation

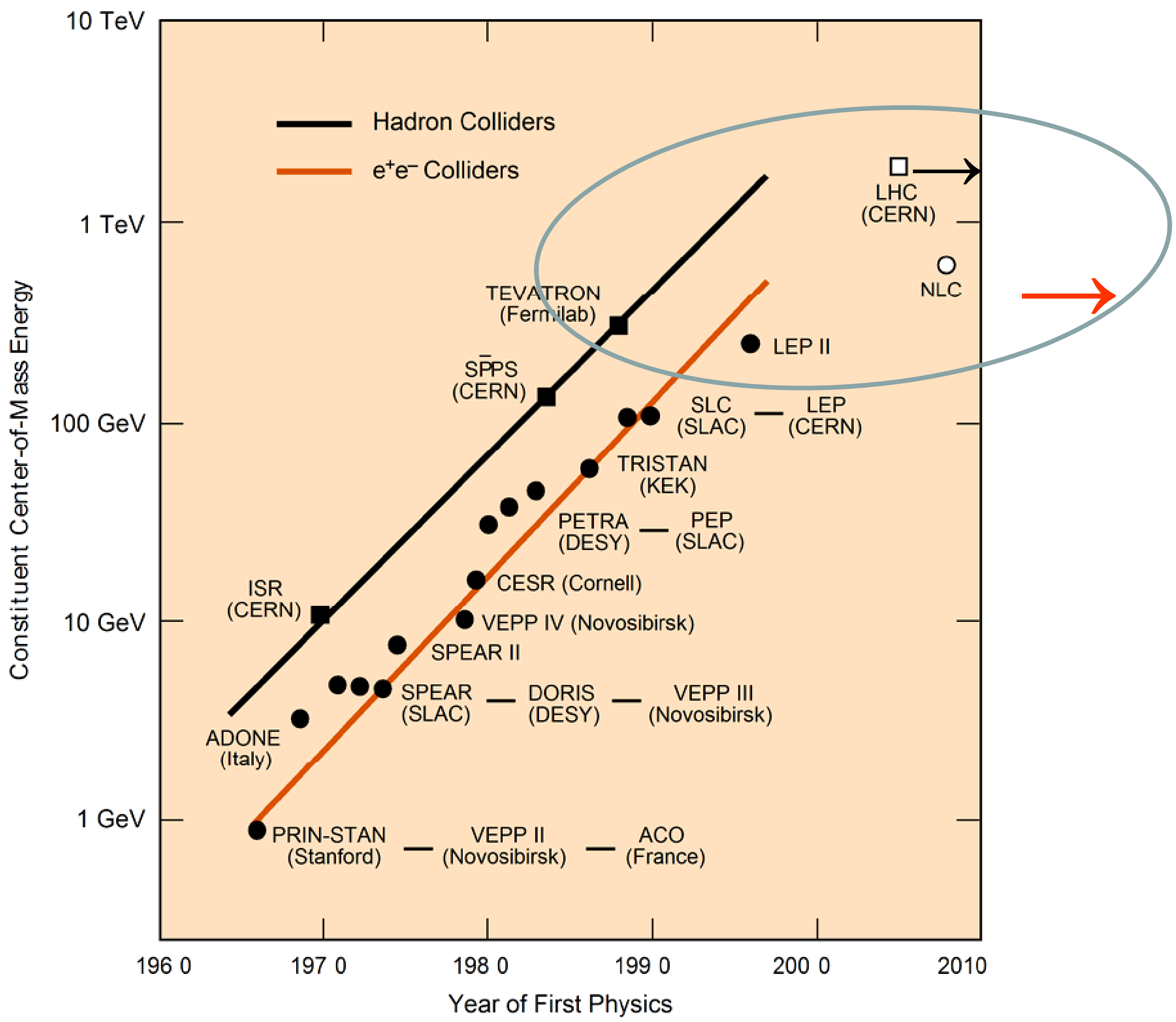

(Suzuki, 2009)

(http://tesla.desy.de/~rasmus/media/Accelerator%20physics/slides/Livingston%20Plot%202.html)

When can we reach 1 PeV ?: Suzuki Challenge

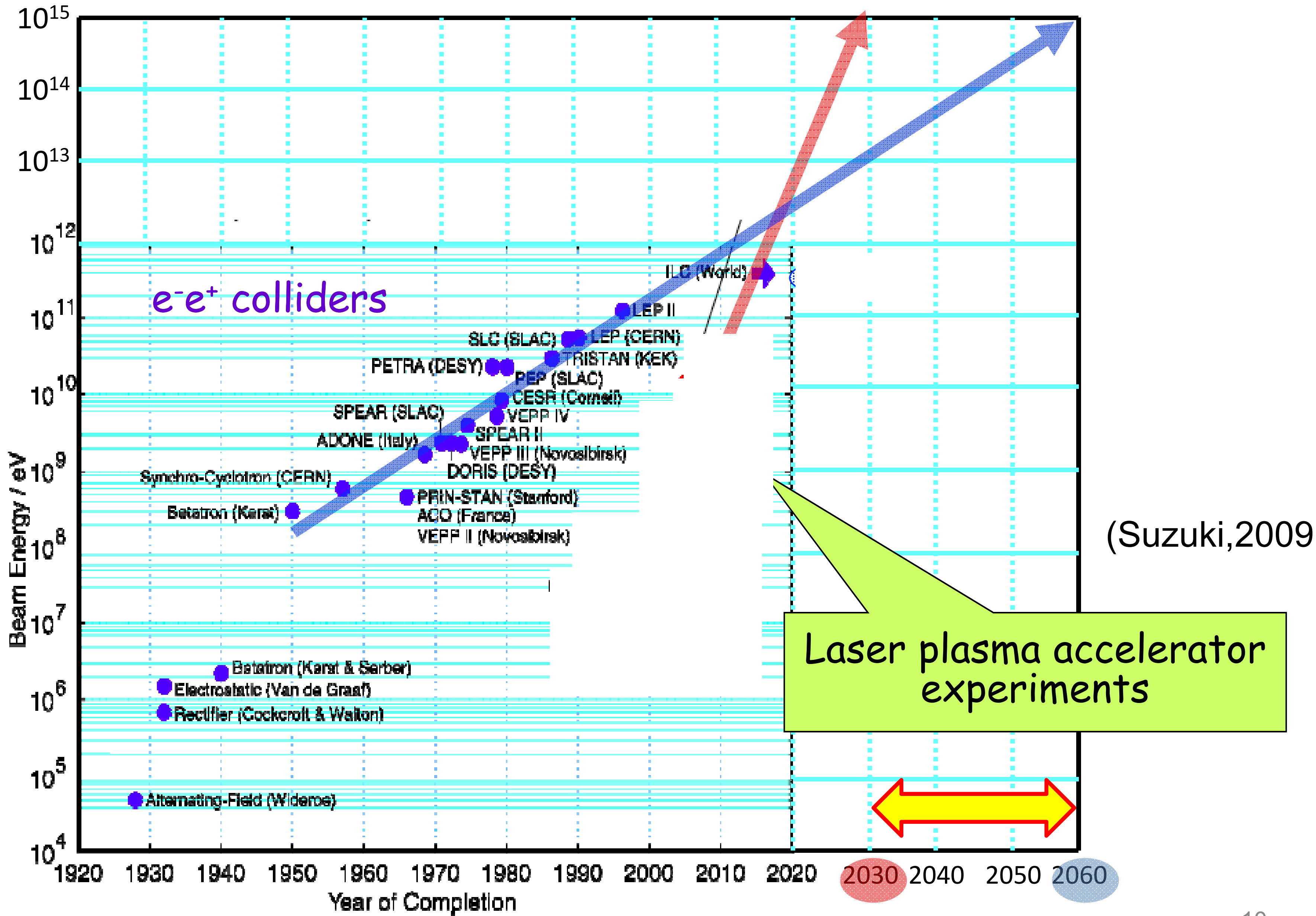

(Suzuki,2009)

V. Yakimenko (BNL) and R. Ischebeck (SLAC), AAC2006 Summary report of WG4

Accelerator

Evolution of Accelerators and their Possibilities (Suzuki,2008)

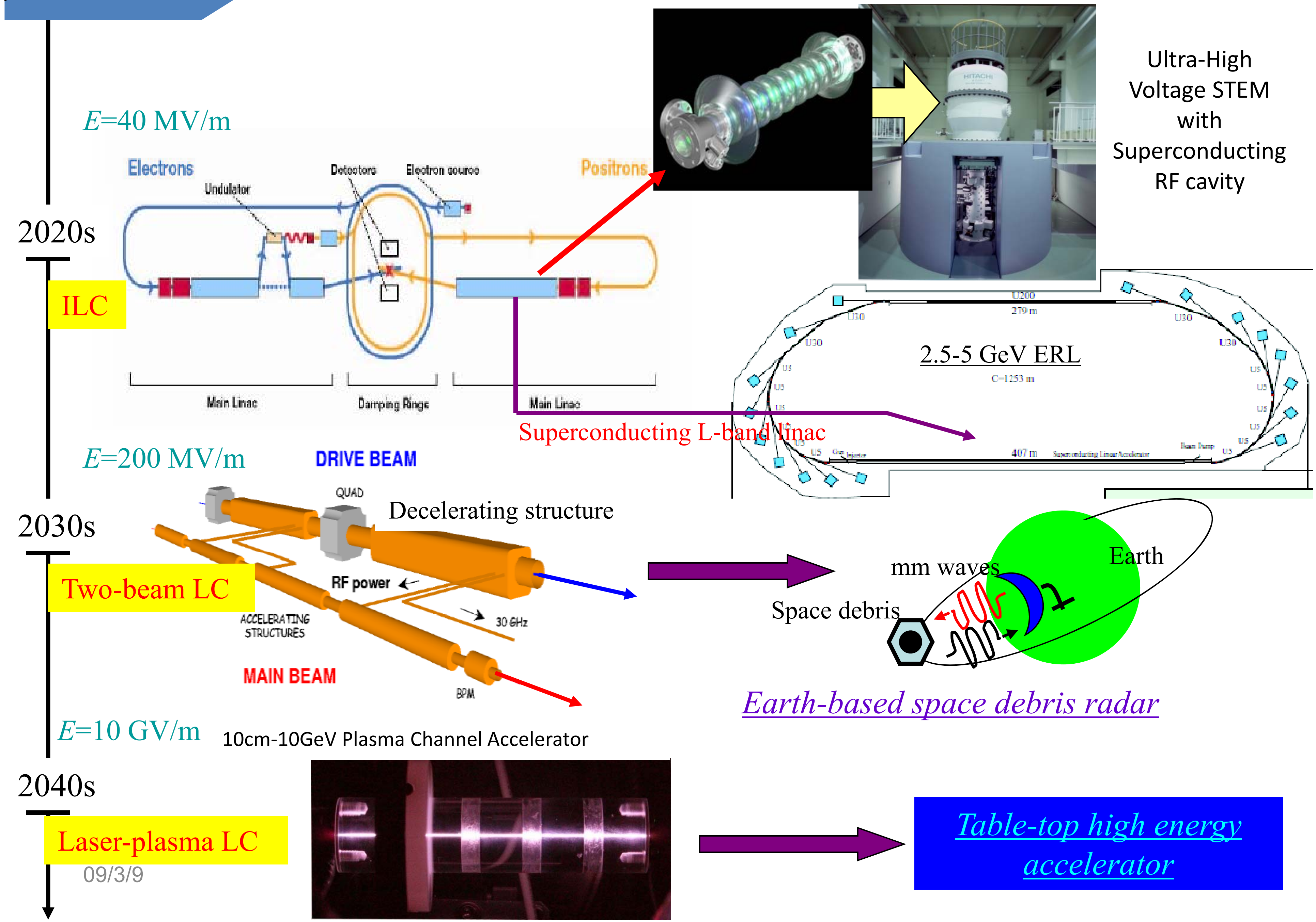

'Bridgelab' goal =
Put *SLAC* on a football field

Initiatives considered, emerging: *CERN, KEK, LBL, DESY, ILE,…*

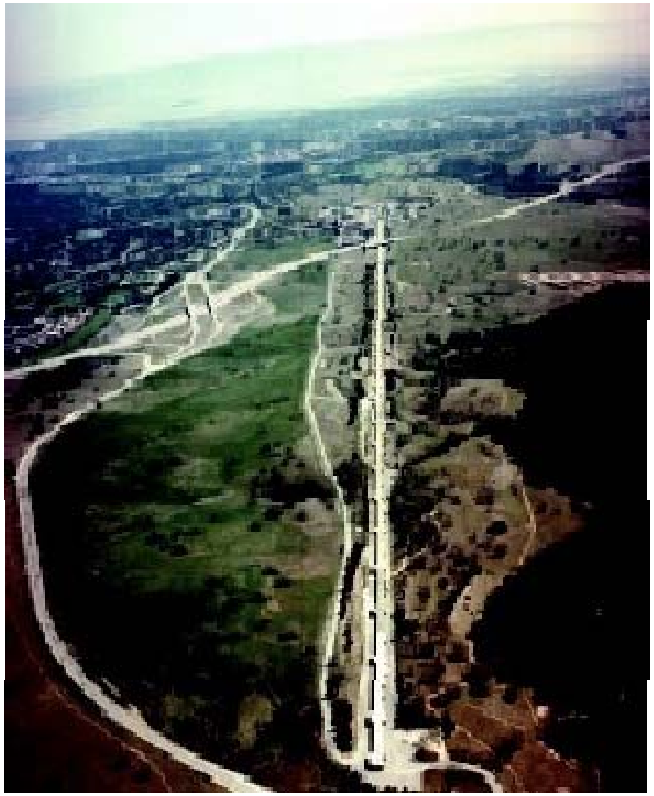

SLAC's 2 mile linac (50GeV)

→

Laser acceleration =

- no material breakdown (→ 3/4 orders higher gradient); however:
- 3 orders finer accuracy, and 2 orders more efficient laser needed

Brief History of *ICUIL* – *ICFA* Joint Effort

- *ICUIL* Chair sounded on A. Wagner (Chair *ICFA*) and Suzuki (incoming Chair) of a common interest in laser driven acceleration, Nov. 2008
- Leemans appointed in November 2008 to lay groundwork for joint standing committee of *ICUIL*
- *ICFA* GA invited Tajima for presentation by *ICUIL* and endorsed initiation of joint efforts on Feb. 13, 2009
- *ICFA* GA endorsed *Joint Task Force*, Aug. 2009
- *Joint Task Force* formed of *ICFA* and *ICUIL* members, W. Leemans, Chair, Sept, 2009
- First Workshop by *Joint Task Force* held @ GSI, Darmstadt, April, 2010
- Report to *ICFA* GA (July,2010) and *ICUIL* GA (Sept, 2010) on the findings
- ‘Bridgelab Symposium’ at L’Orme (Jan., 2011)

Mountain of Lasers
(average power)

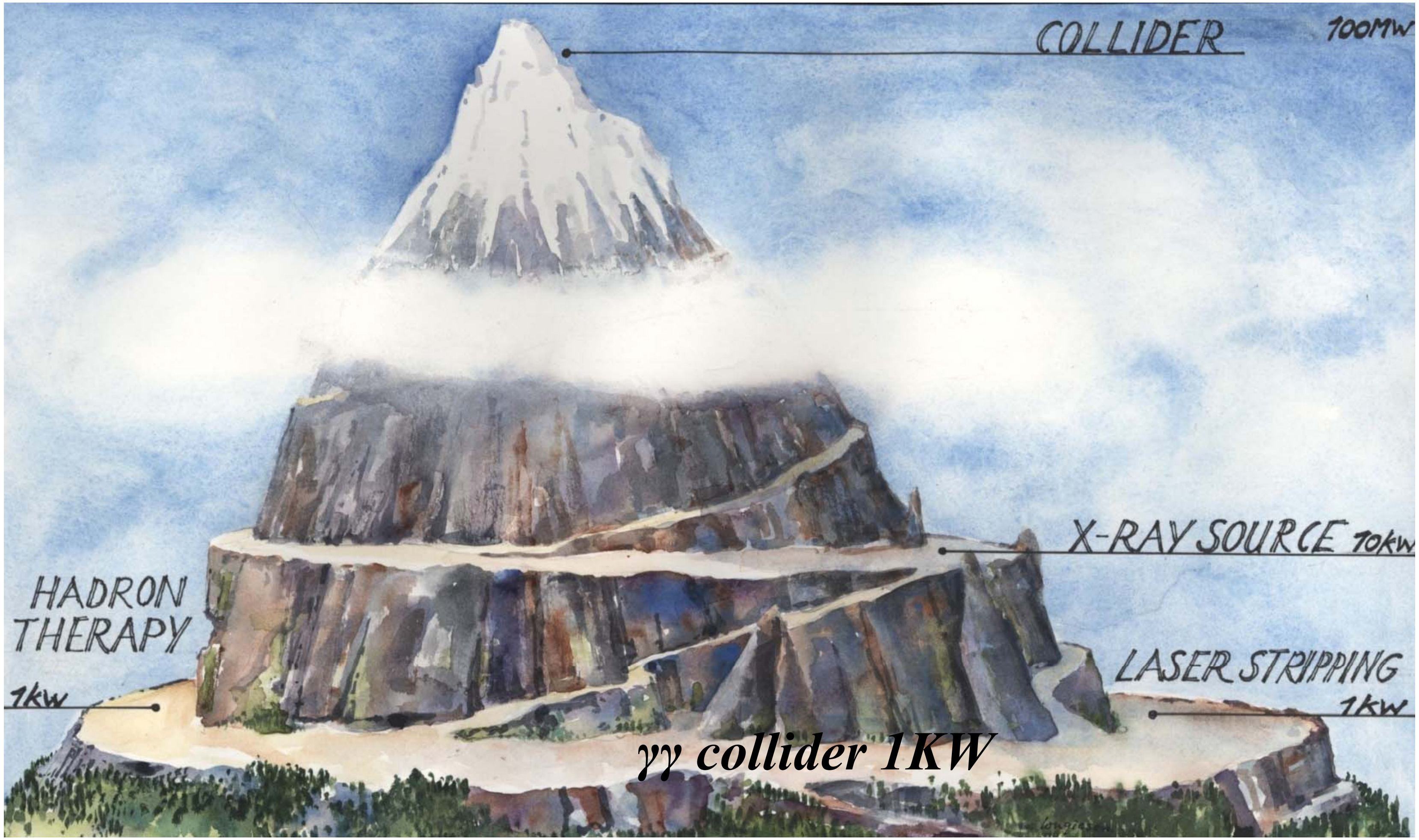

(HEP Examples from *ICFA-ICUIL* JTF)
Friday 6pm Rochester: open JTF

→ average power
→ rep rate
→ pulse shortness

Range of laser parameters

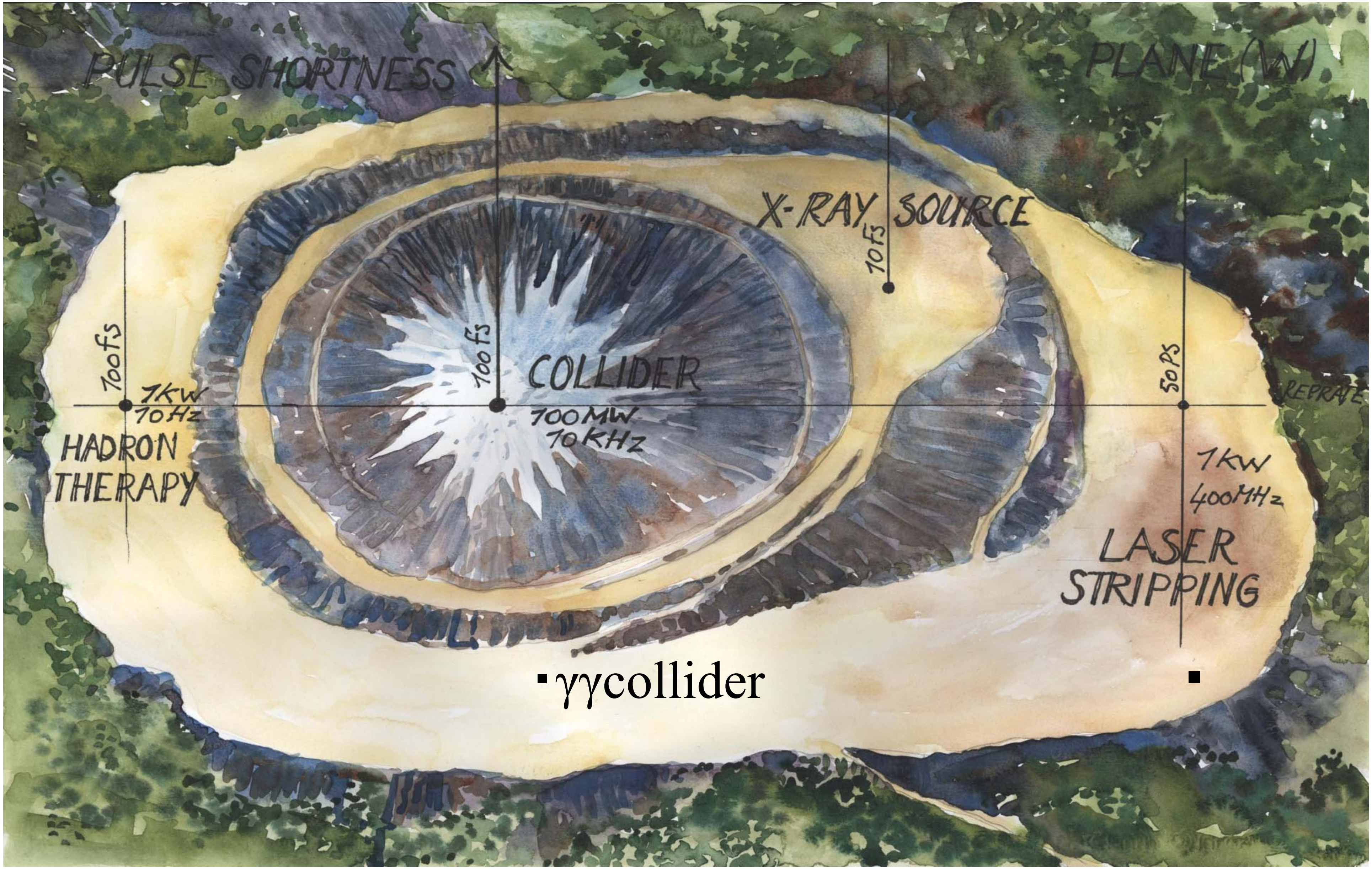

- γγcollider
-

Suggestions to ICFA-ICUIL JTF

- Science efforts by US, Europe, Asia mounting to extend the laser technology toward HEP accelerators
- Technology efforts still lacking in developing suited laser technology(ies) for HEP accelerators
- Technologies: emerging and credible for these
- ICFA-ICUIL collaboration: important guide of direction
- Lead lab(s) necessary to lead and do work on this initiative
- 'Bridgelab' / test facility?
- Other applications important (light sources, medical, nuclear waste management, fusion, defense, etc.)

(Tajima; April 10, 2010)

Laser driven collider concept

a TeV collider

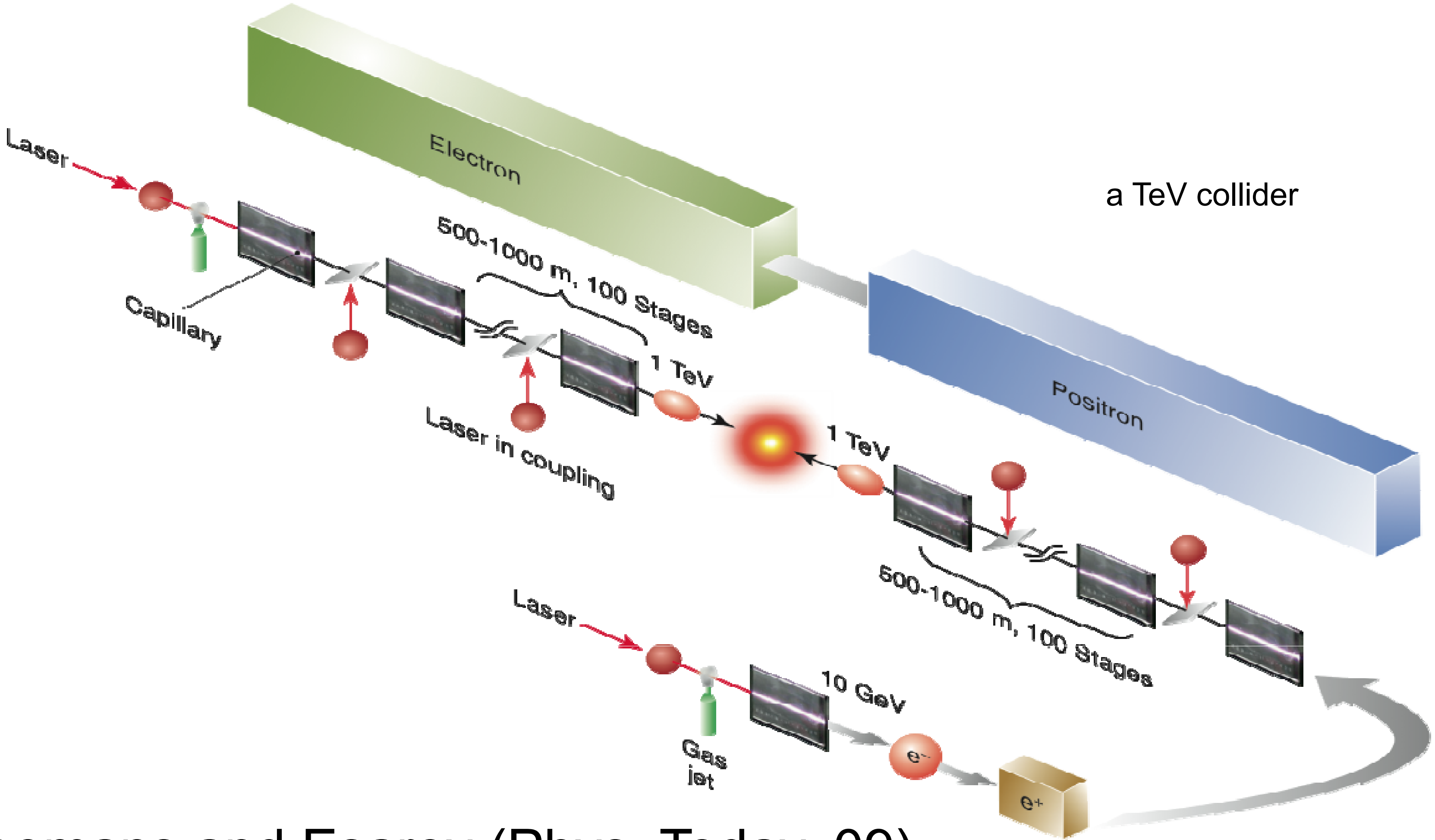

Leemans and Esarey (Phys. Today, 09)
ICFA-ICUIL Joint Task Force on Laser Acceleration(Darmstadt,10)

ICFA-ICUIL Joint Task Force
on laser acceleration (Darmstadt, 2010)

W. Leemans,
Chair of JTF

Case	1 TeV	10 TeV (Scenario I)	10 TeV (Scenario II)
Energy per beam (TeV)	0.5	5	5
Luminosity (10^{34} cm^{-2}s^{-1})	1.2	71.4	71.4
Electrons per bunch ($\times 10^9$)	4	4	1.3
Bunch repetition rate (kHz)	13	17	170
Horizontal emittance $\gamma\varepsilon_x$ (nm-rad)	700	200	200
Vertical emittance $\gamma\varepsilon_y$ (nm-rad)	700	200	200
β^* (mm)	0.2	0.2	0.2
Horizontal beam size at IP σ^*_x (nm)	12	2	2
Vertical beam size at IP σ^*_y (nm)	12	2	2
Luminosity enhancement factor	1.04	1.35	1.2
Bunch length σ_z (μm)	1	1	1
Beamstrahlung parameter Υ	148	8980	2800
Beamstrahlung photons per electron n_γ	1.68	3.67	2.4
Beamstrahlung energy loss δ_E (%)	30.4	48	32
Accelerating gradient (GV/m)	10	10	10
Average beam power (MW)	4.2	54	170
Wall plug to beam efficiency (%)	10	10	10
One linac length (km)	0.1	1.0	0.3

Collider subgroup
List of parameters
(W. Chou)

Table 1
Collider parameters

Laser requirements for such colliders

Case	1 TeV	10 TeV (Scenario I)	10 TeV (Scenario II)
Wavelength (μm)	1	1	1
Pulse energy/stage (J)	32	32	1
Pulse length (fs)	56	56	18
Repetition rate (kHz)	**13**	**17**	**170**
Peak power (TW)	240	240	24
Average laser power/stage (MW)	0.42	0.54	0.17
Energy gain/stage (GeV)	10	10	1
Stage length [LPA + in-coupling] (m)	2	2	0.06
Number of stages (one linac)	50	500	5000
Total laser power (MW)	42	540	1700
Total wall power (MW)	**84**	**1080**	**3400**
Laser to beam efficiency (%) [laser to wake 50% + wake to beam 40%]	20	20	20
Wall plug to laser efficiency (%)	50	50	50
Laser spot rms radius (μm)	69	69	22
Laser intensity (W/cm^2)	3×10^{18}	3×10^{18}	3×10^{18}
Laser strength parameter a_0	1.5	1.5	1.5
Plasma density (cm^{-3}), with tapering	10^{17}	10^{17}	10^{18}
Plasma wavelength (μm)	105	105	33

What is the optimum plasma density?

(Nakajima, 2011)

The electron plasma frequency: $$\omega_p = \sqrt{\frac{4\pi e^2 n_0}{m_e}} = \frac{2\pi c}{\lambda_p}$$

• Plasma electron density n_0 corresponds to frequency of RF cavity, which characterizes accelerator performance .

• Minimizing the overall length of LPA linac

$$L_{total} = \left[L_{stage} + L_c\right]\frac{E_b}{W_{stage}}$$

E_b : the final beam energy
W_{stage} : the energy gain in a single stage
L_{stage} : the single stage plasma length
L_c : the required coupling distance

$$W_{stage} \propto E_z L_d \propto n_0^{-1} \quad L_{stage} \approx L_{pd} \propto n_0^{-3/2}$$

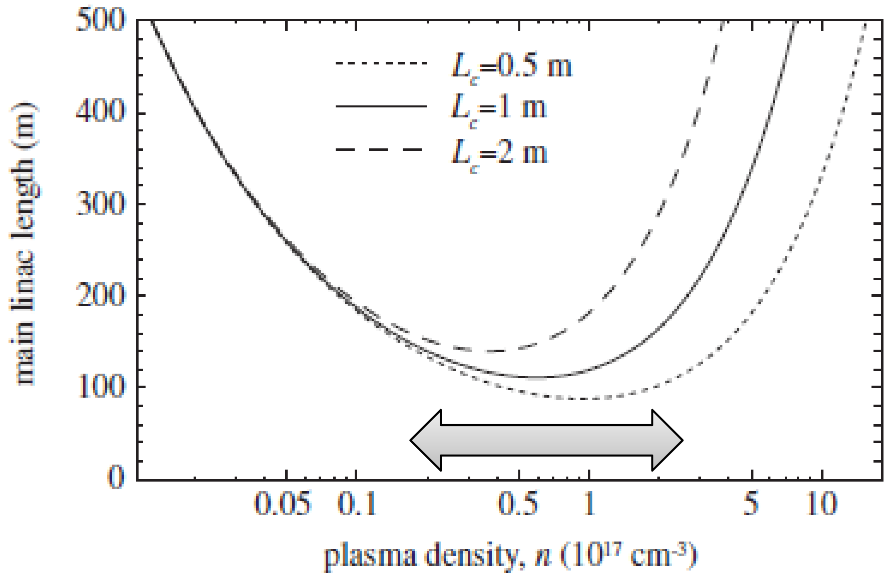

C. B. Schroeder et al., PRST-AB 13, 101301 (2010)

For E_b =0.5 TeV, a_0 =1.5, coupling distance $L_c \lesssim$ 1m

The required operation plasma density ≈ 10^{17} cm^{-3}

• With minimization condition $L_c \sim L_{stage} \approx L_{pd}$

$$L_{total} \propto L_{pd} N_{stage} \propto n_0^{-1/2}$$

• Plasma density is continuously tunable over the broad range.
• Plasma accelerator structure is not so expensive.

Selection of plasma density
is not a big issue.

Plasma density determined by beam quality and power requirement

(Nakajima, 2011)

Radiation damping effect

- Electrons accelerated by LPA undergo betatron oscillations due to strong focusing force
- Emission of synchrotron radiation results in a energy loss and radiation damping with its rate.

$$P_x \cong \frac{2e^2\gamma^2}{3m^2c^3}F_\perp^2 \qquad \nu_\gamma = \frac{P_s}{\gamma mc^2} = \frac{\tau_R \gamma}{m^2c^2}F_\perp^2$$

where $\tau_R = 2r_e/3c \cong 6.26\times10^{-24}$ s

$r_e = e^2/mc^2 = 2.818\times10^{-13}$ cm

$$F_\perp = -mc^2K^2x$$
$$K^2 = 2x_c^{-2}\left(e\phi_0/mc^2\right)$$

for the linear regime with potential ϕ_0, characteristic channel width x_c

$$K = k_p/\sqrt{2}$$

for the blowout (or bubble) regime

Power requirement for the linear collider

- Collision frequency: $f \propto N^{-2} \propto n_0$ for a constant required luminosity
- Beam power: $P_b = fNE_b \propto n_0^{1/2}$
- Average laser power per stage: $P_{avg} \cong fU_L \sim f\cdot P_L\tau_L \propto n_0 \cdot n_0^{-1} \cdot n_0^{-1/2} \propto n_0^{-1/2}$
- Total wall plug power $P_{wall} \propto N_{stage}P_{avg} \propto n_0^{1/2}$

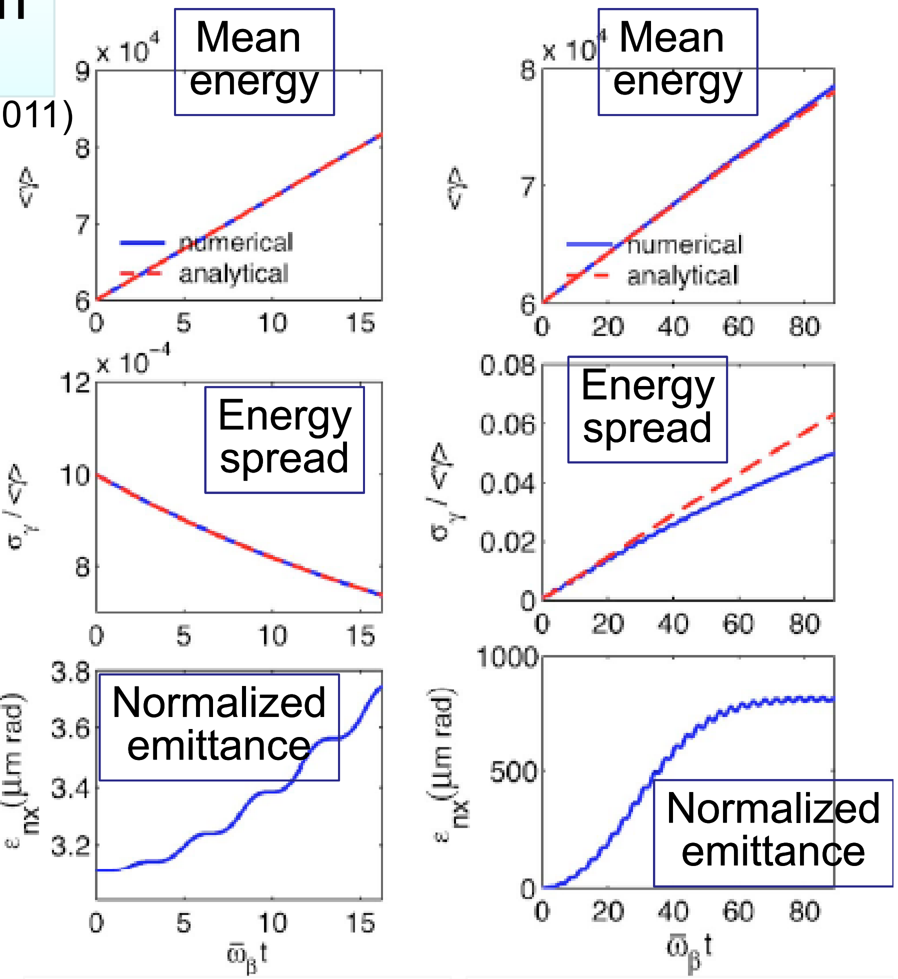

30 GeV injection	30 GeV injection
30 cm plasma channel	30 cm plasma channel
E_z = 37 GV/m	E_z = 37 GV/m
$n_0 = 10^{16}$ cm^{-3}	$n_0 = 3\times10^{17}$ cm^{-3}

P. Michel et al., PRE 74, 026501

From points of high quality and power cost, choose plasma density of the order of 10^{16} cm^{-3}

Design of multi-stage LWFA toward 100 GeV

(Nakajima, 2011)

	Electron Injector	Positron Injector	10 GeV stage	100 GeV stage	Multi-stage 100 GeV	LBNL-BELLA 10 GeV
Energy gain ΔW [GeV]	10	1.8	10	100	10 x 10	10
Laser intensity a_0	2.0	5.5	1.0	2.0	1.0	1.4
Spot radius w_0 [μm]	31	10	64	80	64	90
Pulse duration τ_L [fs]	68	20	120	216	120	95
Peak power P [TW}	130	100	137	865	10 x 137	563
Pulse energy E_L [J]	9	2	16	187	10 x 16	53
Plasma density n_e [cm^{-3}]	2.4 x 10^{17}	5 x 10^{19}	2.8 x 10^{16}	2.4 x 10^{16}	2.8 x 10^{16}	1.0x10^{17}
Plasma length L_p [cm]	15	0.1	200	470	10 x 200	~100
Maximum charge Q [nC]	0.46	1	0.2	2		0.3

∗Stage energy gain of 10-100 GeV would be necessary for 1 – 10 TeV collider application

Issues for LWFA Collider

- Collider Physics issues (what is unique and challenging to LWFA)
  - strong acceleration (compactness)
  - small emittance (strong beam)
  - strong transverse force/large betatron oscillations
  - large quantum beamstrahlung effects
  - miniature finesse issues
- Driver issues (high rep rate, high average power lasers)

First LWFA Collider Study (1997)

Studies of Laser-Driven 5 TeV e^+e^- Colliders in Strong Quantum Beamstrahlung Regime

M. Xie[1], T. Tajima[2], K. Yokoya[3] and S. Chattopadhyay[1]

[1] *Lawrence Berkeley National Laboratory, USA*
[2] *University of Texas at Austin, USA*
[3] *KEK, Japan*

Abstract.

We explore the multidimensional space of beam parameters, looking for preferred regions of operation for a e^+e^- linear collider at 5 TeV center of mass energy. Due to several major constraints such a collider is pushed into certain regime of high beamstrahlung parameter, Υ, where beamstrahlung can be suppressed by quantum effect. The collider performance at high Υ regime is examined with IP simulations using the code CAIN. Given the required beam parameters we then discuss the feasibility of laser-driven accelerations. In particular, we will discuss the capabilities of laser wakefield acceleration and comment on the difficulties and uncertainties associated with the approach. It is hoped that such an exercise will offer valuable guidelines for and insights into the current development of advanced accelerator technologies oriented towards future collider applications.

INTRODUCTION

It is believed that a linear collider at around 1 TeV center of mass energy can be built more or less with existing technologies. But it is practically impossible to go much beyond that energy without employing a new, yet largely unknown method of acceleration. However, apart from knowing the details of the future technologies, certain collider constraints on electron and positron beam parameters are considered to be quite general and have to be satisfied, e.g. available wall plug power and the constraints imposed by collision processes: beamstrahlung, disruption, backgrounds, etc. Therefore it is appropriate to explore and chart out the preferred region in parameter space based on these constraints, and with that hopefully to offer valuable guide-

With a plasma density of 10^{17}cm^{-3}, such a gradient can be produced in the linear regime with more or less existing T^3 laser, giving a plasma dephasing length of about 1 m [13]. If we assume a plasma channel tens of μm in width can be formed at a length equals to the dephasing length, we would have a 10 GeV acceleration module with an active length of 1 m. Of course, creating and maintaining a plasma channel of the required quality is no simple matter. To date, propagation in a plasma channel over a distance of up to 70 Rayleigh lengths (about 2.2 cm) of moderately intense pulse ($\sim 10^{15}\text{W/cm}^2$) has been demonstrated [14]. New experiment aiming at propagating pulses with intensities on the order of 10^{18}W/cm^2 (required for a gradient of 10 GeV/m) is underway [13].

Table 1. Beam Parameters at Three Values of Beam Power

CASE	P_b(MW)	$N(10^8)$	f_c(kHz)	ε_y(nm)	$\beta_y(\mu\text{m})$	σ_y(nm)	$\sigma_z(\mu\text{m})$
I	2	0.5	50	2.2	22	0.1	0.32
II	20	1.6	156	25	62	0.56	1
III	200	6	416	310	188	3.5	2.8

Table 2. Results Given By the Formulas

CASE	Υ	D_y	F_{oide}	n_γ	δ_E	n_p	$\mathcal{L}_g(10^{35}\text{cm}^{-2}\text{s}^{-1})$
I	3485	0.93	0.89	0.72	0.2	0.19	1
II	631	0.29	0.89	0.72	0.2	0.12	1
III	138	0.081	0.91	0.72	0.2	0.072	1

Table 3. Results Given By CAIN Simulations

CASE	n_γ	δ_E	σ_e/E_0	n_p	$\mathcal{L}/\mathcal{L}_g(\text{W}_{\text{cm}} \in 1\%)$	$\mathcal{L}/\mathcal{L}_g(\text{W}_{\text{cm}} \in 10\%)$
I	1.9	0.38	0.42	0.28	0.83	1.1
II	0.97	0.26	0.36	0.12	0.65	0.80
III	0.84	0.21	0.32	0.06	0.62	0.75

Although a state-of-the-art T^3 laser, capable of generating sub-ps pulses with 10s of TW peak power and a few Js of energy per pulse [11], could almost serve the need for the required acceleration, the average power or the rep rate of a single unit is still quite low, and wall-plug efficiency inadequate. In addition, injection scheme and synchronization of laser and electron pulse from

Xie et al. AAC Conference Proc. (1997)

Also, Chattopadhay et al., Snowmass (1996)

Collider Physics I

Basic parameters and scalings of LWFA Collider in Maximizing luminosity with constraintsof beamstrahlung , disruption, and γ emission

$$f_c = \left(\frac{P_b}{E_{cm}}\right)\left(\frac{1}{N}\right) \quad (1)$$

$$\sigma_y = \left(\frac{1}{\sqrt{4\pi}}\right)\left(\frac{1}{\sqrt{R}}\right)\left(\sqrt{\frac{P_b}{E_{cm}\mathcal{L}_g}}\right)\left(\sqrt{N}\right)$$

$$\Upsilon = \left(\frac{5\sqrt{\pi}r_e^2}{6\alpha mc^2}\right)\left(\frac{\sqrt{R}}{1+R}\right)\left(\sqrt{\frac{E_{cm}^3\mathcal{L}_g}{P_b}}\right)\left(\frac{\sqrt{N}}{\sigma_z}\right)$$

$$D_y = \left(16\pi mc^2 r_e\right)\left(\frac{R}{1+R}\right)\left(\frac{\mathcal{L}_g}{P_b}\right)(\sigma_z)$$

$$n_\gamma = 2.54U_0(\Upsilon)F\,, \quad \delta_E = 1.24\Upsilon U_1(\Upsilon)F \quad (5)$$

$$F = \left(\frac{5\sqrt{\pi}r_e^2}{3\lambda_c}\right)\left(\frac{\sqrt{R}}{1+R}\right)\left(\sqrt{\frac{E_{cm}\mathcal{L}_g}{P_b}}\right)\left(\sqrt{N}\right). \quad (6)$$

$$f_c \sim 1/N\,, \quad \sigma_y \sim \sqrt{N}\,, \quad D_y \sim \sigma_z\,, \quad \Upsilon \sim \sqrt{N}/\sigma_z \quad (7)$$

$$n_\gamma \sim U_0(\Upsilon)\sqrt{N}\,, \quad \delta_E \sim \Upsilon U_1(\Upsilon)\sqrt{N}. \quad (8)$$

In the limit $\Upsilon \gg 1$, $U_0(\Upsilon) \to 1/\Upsilon^{1/3}$, $\Upsilon U_1(\Upsilon) \to 1/\Upsilon^{1/3}$. Eq.(8) becomes

$$n_\gamma \sim (N\sigma_z)^{1/3}\,, \quad \delta_E \sim (N\sigma_z)^{1/3}. \quad (9)$$

First paper on LWFA collider
Xie, M., Tajima, T., Yokoya, K. and Chattopadyay, S., *Studies of Laser-Driven 5TeV e+e- Colliders in Strong Quantum Beamstrahlung Regime*, (AIP Conference Proceedings, New York, 1997), **398**, p. 233-242.

Collider Physics II

Xie et al (1997)

Optimization for LWFA Collider at IP

Collision parameter dependence

Collision energy spectrum

First LWFA Collider design

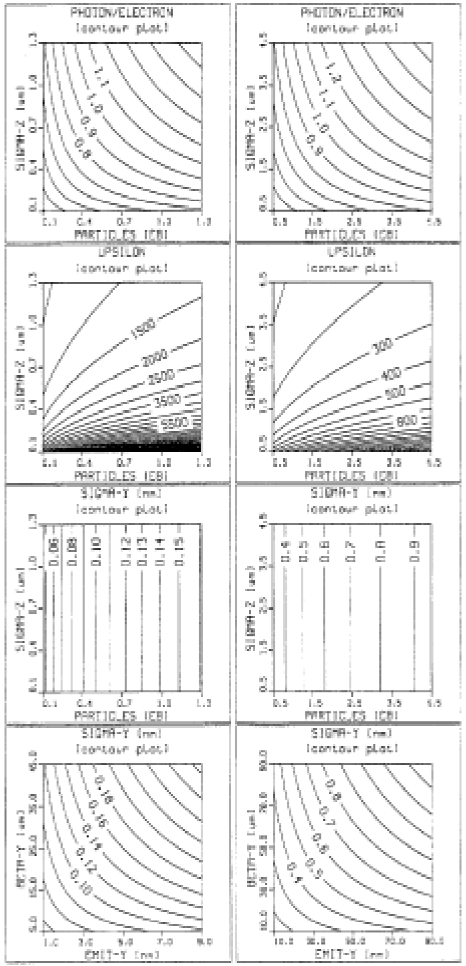

FIGURE 1. Parameter scans for P_b = 2MW (column 1) and 20MW (column 2).

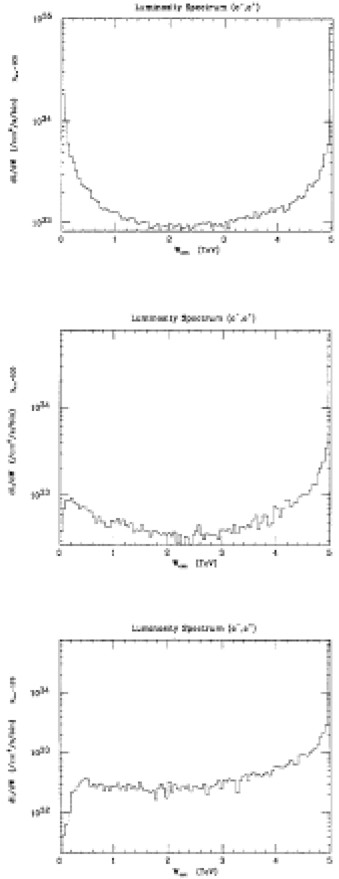

e^+e^- luminosity spectrum for case I (top), II (middle), III (bottom)

Table 1. Beam Parameters at Three Values of Beam Power

CASE	P_b(MW)	$N(10^8)$	f_c(kHz)	ϵ_y(nm)	$\beta_y(\mu m)$	σ_y(nm)	$\sigma_z(\mu m)$
I	2	0.5	50	2.2	22	0.1	0.32
II	20	1.6	156	25	62	0.56	1
III	200	6	416	310	188	3.5	2.8

Table 2. Results Given By the Formulas

CASE	Υ	D_y	F_{hide}	n_γ	δ_E	n_p	$\mathcal{L}_g(10^{35}\mathrm{cm}^{-2}\mathrm{s}^{-1})$
I	3485	0.93	0.89	0.72	0.2	0.19	1
II	631	0.29	0.89	0.72	0.2	0.12	1
III	138	0.081	0.91	0.72	0.2	0.072	1

Table 3. Results Given By CAIN Simulations

CASE	n_γ	δ_E	σ_ϵ/E_0	n_p	$\mathcal{L}/\mathcal{L}_g(W_{cm} \in 1\%)$	$\mathcal{L}/\mathcal{L}_g(W_{cm} \in 10\%)$
I	1.9	0.38	0.42	0.28	0.83	1.1
II	0.97	0.26	0.36	0.12	0.65	0.80
III	0.84	0.21	0.32	0.06	0.62	0.75

Physics under extremely strong **quantum beamstrahlung regime** $\Upsilon >> 1$ (the shorter the bunch, the smaller Υ)

Collider Physics III

LWFA properties under multistage collider design
First multistage model for LWFA collider

PHYSICAL REVIEW SPECIAL TOPICS - ACCELERATORS AND BEAMS, VOLUME 3, 071301 (2000)

Particle dynamics in multistage wakefield collider

S. Cheshkov, T. Tajima,* and W. Horton
Department of Physics and Institute for Fusion Studies, The University of Texas at Austin, Austin, Texas 78712

K. Yokoya
KEK National Laboratory for High Energy Physics, Tsukuba-Shi, Japan
(Received 24 January 2000; published 27 July 2000)

The dynamics of particles in laser pulse-driven wakefields over multistages in a collider is studied. A map of phase space dynamics over a stage of wakefield acceleration induced by a laser pulse (or electron beam) is derived. The entire system of a collider is generated with a product of multiple maps of wakefields, drifts, magnets, etc. This systems map may include offsets of various elements of the accelerator, representing noise and errors arising from the operation of such a complex device. We find that an unmitigated strong focusing of the wakefield coupled with the alignment errors of the position (or laser beam aiming) of each wakefield stage and the unavoidable dispersion in individual particle betatron frequencies leads to a phase space mixing and causes a transverse emittance degradation. The rate of the emittance increase is proportional to the number of stages, the energy of the particles, the betatron frequency, the square of the misalignment amplitude, and the square of the betatron phase shift over a single stage. The accelerator with a weakened focus in a channel can, therefore, largely suppress the emittance degradation due to errors.

PACS numbers: 52.40.Nk, 52.65.Cc, 52.75.Di, 05.40.−a

I. INTRODUCTION

The use of plasma waves excited by laser beams for electron acceleration was proposed by Tajima and Dawson [1].

$$\mathcal{L} = \frac{f_c N^2}{4\pi\sigma_x\sigma_y} = \frac{\gamma f_c N^2}{4\pi\sqrt{\epsilon_x\beta_x^*}\sqrt{\epsilon_y\beta_y^*}}, \qquad (1)$$

where f_c is the collision frequency, N is the particle num-

Collider Physics IV

LWFA model for collider

Stage accelerator matrix

$$\frac{d\gamma}{dz} = k_p \Phi_0 \cos(\Psi), \quad (19)$$

$$\frac{d\Psi}{dz} = \frac{k_p}{2\gamma_p^2}. \quad (20)$$

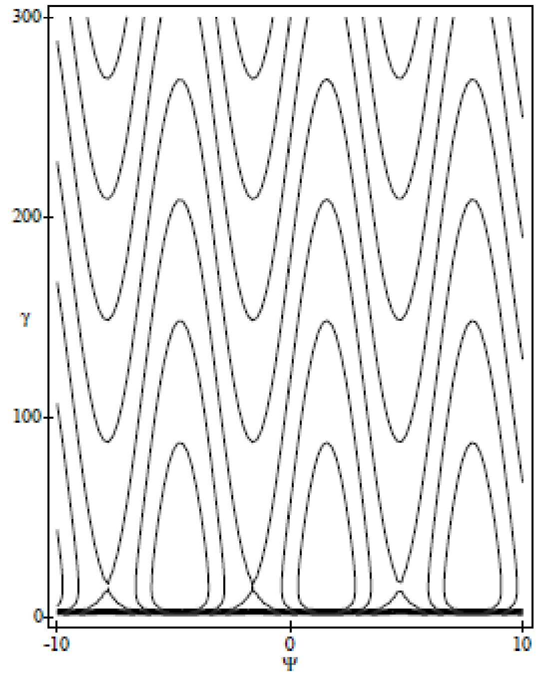

FIG. 1. The longitudinal phase space: electron Lorenz factor γ vs its phase with respect to the wakefield Ψ. The parameters used were $\gamma_p = 15$, $\Phi_0 = 0.2$.

Cheshkov et al (2000)

Longitudinal dynamics

The linearized equations of motion for the longitudinal degrees of freedom are

$$\delta\Psi_{n+1} = \delta\Psi_n, \quad (23)$$

$$\delta\gamma_{n+1} = 2\gamma_p^2\Phi_0[\cos(\Psi_s + \Delta) - \cos(\Psi_s)]\delta\Psi_n + \delta\gamma_n, \quad (24)$$

Transeverse dynamics

$$\ddot{u} + \Big[\omega_\beta^2 \sin(\omega_s z + \Psi_s + \delta\Psi_n) - \frac{1}{2}\frac{\ddot{\gamma}}{\gamma} + \frac{1}{4}\frac{\dot{\gamma}^2}{\gamma^2}\Big]\tilde{u} = 0, \quad (25)$$

where

$$\omega_s = \frac{k_p}{2\gamma_p^2}, \quad (26)$$

$$\omega_\beta = \left(\frac{4\Phi_0}{\gamma r_s^2}\right)^{1/2} \quad (27)$$

$$M = \begin{pmatrix} \cos(\frac{\omega}{\omega_s}\Delta) & \frac{1}{\omega}\sin(\frac{\omega}{\omega_s}\Delta) \\ -\omega\sin(\frac{\omega}{\omega_s}\Delta) & \cos(\frac{\omega}{\omega_s}\Delta) \end{pmatrix} \begin{pmatrix} 1 & L \\ 0 & 1 \end{pmatrix}, \quad (29)$$

where L is the drift distance between the wakefield stages and $1/\omega$ is the betatron length in the wakefield. The matrix (29) may be also written as

$$M = \begin{pmatrix} \cos(\frac{\omega}{\omega_s}\Delta) & \frac{1}{\omega}\sin(\frac{\omega}{\omega_s}\Delta) + L\cos(\frac{\omega}{\omega_s}\Delta) \\ -\omega\sin(\frac{\omega}{\omega_s}\Delta) & -L\omega\sin(\frac{\omega}{\omega_s}\Delta) + \cos(\frac{\omega}{\omega_s}\Delta) \end{pmatrix}. \quad (30)$$

The transverse map $\mathcal{M}$ for the whole accelerator system is

$$\mathcal{M} = M^N, \quad (31)$$

Collider Physics V

Cumulative effects over multistages

Strong LWFA betatron oscillations lead to emittance degradation

severe transverse emittance growth. Basically, what
ens is that the particles rotate at different angular ve-
ies in the transverse phase space and, if there is a
position shift present, we get a characteristic banana-
ed distribution (see Fig. 3c) (it is banana shaped only
e dislocation size is larger than the beam size, but in
case the particle distribution gets diluted because of
nisalignments). This process critically depends on the
nitude of the betatron frequency spread. This means
the typical strength of the focusing force is of great
ortance. Of course, additional information can be ex-
ed from the other total phase space cross sections; see
4. However, here we concentrate on the transverse
tance as a figure of merit due to its importance to the
luminosity of the collider. The effect of plasma noise
other noise, such as laser or the boundary) on the par-
dynamics over a stage may also be incorporated in a

$$\begin{pmatrix}\tilde{x}_{n+1}\\ \dot{\tilde{x}}_{n+1}\end{pmatrix} = M_n\begin{pmatrix}\tilde{x}_n - \tilde{\mathcal{D}}_n\\ \dot{\tilde{x}}_n\end{pmatrix} + \begin{pmatrix}\tilde{\mathcal{D}}_n\\ 0\end{pmatrix}, \qquad (34)$$

where $\mathcal{D}_n$ is the stochastic misalignment ($\tilde{\mathcal{D}}_n = \sqrt{\gamma_n}\,\mathcal{D}_n$). The longitudinal degrees of freedom are not affected. For this map to describe realistically the electron motion, we assume that $\sigma_{\mathcal{D}} \ll r_s$. The total transverse map (in the presence of errors) can be written in the form

$$\begin{pmatrix}\tilde{x}_{n+1}\\ \dot{\tilde{x}}_{n+1}\end{pmatrix} = M_n M_{n-1}\cdots M_2(1-M_1)\begin{pmatrix}\tilde{\mathcal{D}}_1\\ 0\end{pmatrix} + \cdots(1-M_n)\begin{pmatrix}\tilde{\mathcal{D}}_n\\ 0\end{pmatrix} + M_n M_{n-1}\cdots M_1\begin{pmatrix}\tilde{x}_1\\ \dot{\tilde{x}}_1\end{pmatrix}. \qquad (35)$$

$$\langle \mathcal{D}\rangle = 0, \qquad (38)$$

$$\langle \mathcal{D}(z_1)\mathcal{D}(z_2)\rangle = \sigma_{\mathcal{D}}^2 l\,\delta(z_1 - z_2). \qquad (39)$$

Applying the theory of random walk of a harmonic oscillator driven by a random force, we obtain

$$\langle \tilde{x}\rangle = 0, \qquad \langle \dot{\tilde{x}}\rangle = 0, \qquad \langle \tilde{x}\dot{\tilde{x}}\rangle = 0, \qquad (40)$$

$$\langle \tilde{x}^2\rangle = Dz = DNl, \qquad \langle \dot{\tilde{x}}^2\rangle = D\omega^2 z, \qquad (41)$$

where the diffusion coefficient D is given by

$$D = \frac{1}{2}\gamma\,\omega^2 l\,\sigma_{\mathcal{D}}^2. \qquad (42)$$

We are also assuming that the emittance growth is large (compared to the initial emittance). So, using (40) and (41), we obtain

$$\Delta\epsilon \approx \omega D\,z = \frac{1}{2}\gamma\omega(\omega l)^2\sigma_{\mathcal{D}}^2 N. \qquad (43)$$

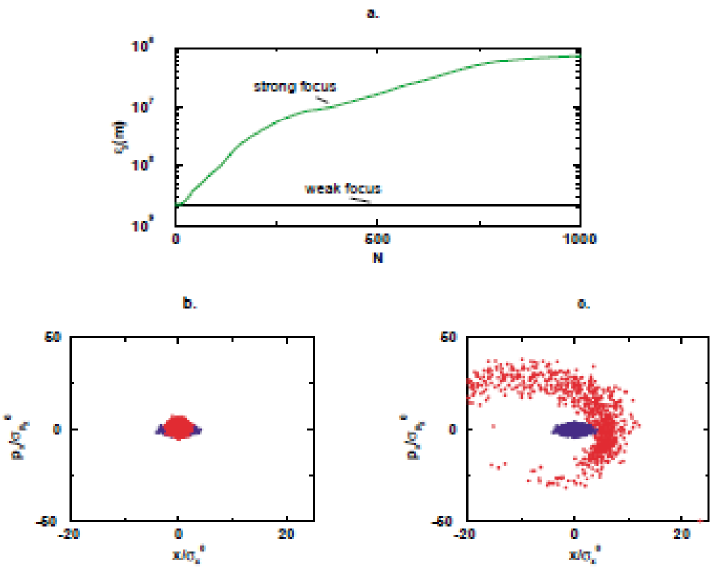

$$\Delta\epsilon \approx \frac{1}{2}\gamma\omega(\omega l)^2\sigma_{\mathcal{D}}^2\left(\frac{\gamma}{\Delta\gamma}\right)^{1/2}\sqrt{N\ln\left(1+\frac{\Delta\gamma N}{\gamma}\right)}, \qquad (44)$$

where γ is the initial particle energy. Typically, $\Delta\gamma \approx a_0^2 E_0 l$ and $\omega \propto \frac{a_0}{r_s}$, so we obtain

$$\Delta\epsilon \propto \frac{l^{3/2}a_0^2\sigma_{\mathcal{D}}^2}{r_s^3 E_0^{1/2}}\sqrt{N\ln\left(1+\frac{\Delta\gamma N}{\gamma}\right)}. \qquad (45)$$

Cheshkov et al (2000)

Collider Physics VI

Optimization for LWFA collider
Strategy of synchronous orbit operation

PHYSICAL REVIEW SPECIAL TOPICS - ACCELERATORS AND BEAMS, VOLUME 3, 101301 (2000)

High energy laser-wakefield collider with synchronous acceleration

C. Chiu,[1] S. Cheshkov,[1] and T. Tajima[1,2]
[1]*Department of Physics, University of Texas at Austin, Austin, Texas 78712*
[2]*Lawrence Livermore National Laboratory, Livermore, California 94550*
(Received 5 May 2000; published 23 October 2000)

A recent study on a high energy accelerator system which involves multistage laser wakefield acceleration shows that the system is very sensitive to jitters due to misalignment between the beam and the wakefield. In particular, the effect of jitters in the presence of a strong focusing wakefield and initial phase space spread of the beam leads to severe emittance degradation of the beam. One way to improve the emittance control is to mitigate the wakefield by working with a plasma channel. However, there are limitations in this approach. Our present investigation does not involve a plasma channel. Instead of averaging over the full phase range of the quarter-wave acceleration, we treat the phase range as a variable. We have found that, for a fixed final acceleration energy and a small phase slip, the final emittance is inversely proportional to the total number of stages. This leads us to consider an accelerator system which consists of superunits, where each superunit consists of closely spaced short tubes, or chips, with the wakefield of each chip being created by an independent laser pulse. There is a relatively large gap between adjacent superunits. With this arrangement the beam electrons are accelerated with a small phase slip; i.e., the phase of the beam is approximately synchronous with respect to the wakefield. This system is designed to have resilience against jitters. It has its practical limitations. We also consider a "horn model" with an exact synchronous acceleration based on a scheme suggested by Katsouleas. Computer simulation of both the chip model and the horn model confirms an expected $(\sin\psi)^{3/2}$ law for emittance degradation in the small phase angle region. Thus the choice of a small loading phase together with a small phase slip provides another important ingredient in controlling emittance degradation.

PACS numbers: 52.40.Nk, 52.65.Cc, 52.75.Di, 05.40.−a

Collider Physics VII

optics of the LWFA collider stages

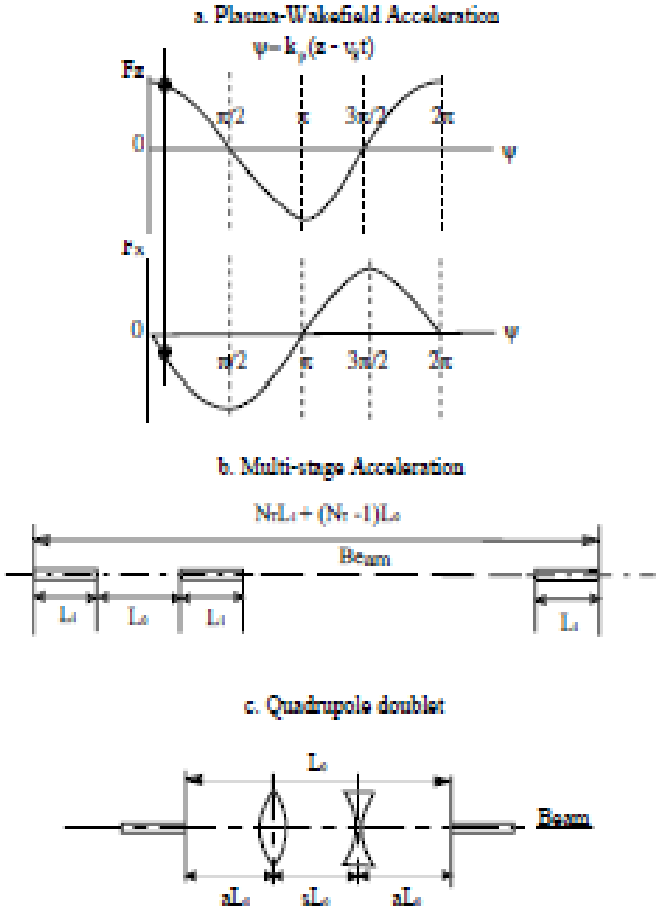

Chiu et al (2000)

Lorentz factor from the nth stage to the $n+1$th stage for a typical particle[2] is given by

$$\gamma_{n+1} = \gamma_n + \Delta\gamma + \frac{\partial\Delta\gamma}{\partial\psi}\delta\psi , \qquad (7)$$

where the increase in the Lorentz factor over an acceleration stage is given by

$$\Delta\gamma = \Delta\gamma_{max}[\sin(\psi_s + \Delta) - \sin\psi_s],$$

with

$$\Delta\gamma_{max} = 2\gamma_p^2\Phi_0 ,$$
$$\frac{\partial\Delta\gamma}{\partial\psi} = \Delta\gamma_{max}[\cos(\psi_s + \Delta) - \cos\psi_s].$$

To the extent that one neglects the order of $\frac{1}{2\gamma_p^2}$, for a typical particle, the deviation of its longitudinal phase from the center of the beam in going from one stage to the next remains fixed; i.e.,

$$\delta\psi_{n+1} = \delta\psi_n = \delta\psi . \qquad (8)$$

C. Transverse iterative map

Transverse equation of motion. For the transverse motion of the beam particles in the x direction, we work with the two variables p_x and x. The equations of motion for these two variables are given by the Lorentz force equation and the definition of momentum,

$$\frac{dp_x}{dz} = \frac{dp_x}{cdt} = -\frac{eE_x}{c} \quad \text{and} \quad \frac{dx}{dz} = \frac{p_x}{m\gamma c} . \qquad (9)$$

It is shown in Ref. [5] that, in terms of the variable $u = \sqrt{\gamma}x$, the transverse force is approximately harmonic. The two equations of motion lead to

[2]Comments on a typical beam particle: Technically we could have introduced beam particle labels, i.e., $i = 1, 2, \ldots, N_0$. Then the ith particle would have a Lorentz factor of $\gamma_i = \gamma_0 + \delta\gamma_i$. Here γ_0 is the Lorentz factor at the "center" of the beam. To be precise, $\delta\gamma_i = \sigma_\gamma\chi_1(i)$ with $\chi_1(i)$ being a random number generated by a Gaussian distribution having a unit width. By the construction here, σ_γ is the Gaussian width, or simply the width, of the variable $\delta\gamma$. For brevity throughout the text we will suppress the beam particle label and refer to, for example, $\gamma = \gamma_0 + \delta\gamma$ as the Lorentz factor for a typical particle which has a width σ_γ. Similarly, the same typical particle will have a longitudinal phase ψ, with a width σ_ψ and a random variable χ_2 from $\{\chi_2(i)\}$. We will also apply the same convention to its transverse coordinates x and x'. They have their widths and the corresponding random variables from the set of $\{\chi_3(i)\}$ and $\{\chi_4(i)\}$.

$$\frac{d^2u}{dz^2} \approx \frac{1}{mc\sqrt{\gamma}}\frac{dp_x}{dz} = -\frac{1}{mc\sqrt{\gamma}}\frac{eE_x}{c} = -\Omega^2 u , \qquad (10)$$

where

$$\Omega^2 = \frac{1}{mc\sqrt{\gamma}}\frac{4e}{c\sqrt{\gamma}r_s^2}\frac{\Phi_0 E_{bk}}{k_p}\sin\psi = \frac{\pi a_0^2}{r_s^2\gamma}\sin\psi . \qquad (11)$$

Jitters and the transverse map. So far the system is Hamiltonian and thus the emittance of the electron beam is preserved. Now consider jitters in the transverse directions, which, as mentioned earlier, may be due to the misalignment at each stage between the wakefield with respect to the beam line. We follow a procedure similar to those for the generation of random phase space variables. At each acceleration stage a random number χ is generated based on a normalized Gaussian distribution with a width unity. Denote the modified jitter displacement in the x direction by $D = \sqrt{\gamma}\sigma_D\chi$. This leads to a following recurrence relation in going from the nth stage to the $n+1$th stage:

$$\begin{pmatrix} u_{n+1} \\ u'_{n+1} \end{pmatrix} = M_{gap}M_{wk}\begin{pmatrix} u_n - D \\ u'_n \end{pmatrix} + \begin{pmatrix} D \\ 0 \end{pmatrix}. \qquad (12)$$

The wakefield acceleration matrix is given by

$$M_{wk} = \begin{bmatrix} \cos\theta & \frac{1}{\Omega}\sin\theta \\ -\Omega\sin\theta & \cos\theta \end{bmatrix}, \qquad \theta = \Omega L_1 . \qquad (13)$$

Here L_1 is the spatial interval of acceleration, which is the tube length; see Fig. 1(b). From Eq. (6), $L_1 = 2\gamma_p^2\Delta_1/k_p$, where Δ_1 is the phase slip over the corresponding spatial interval. For a gap with a free space interval L_0, the corresponding transport matrix is given by

$$M_{gap} = S(L) = \begin{bmatrix} 1 & L \\ 0 & 1 \end{bmatrix}. \qquad (14)$$

Magnets. It is well known that the presence of magnets increases the stability of electron orbits. Figure 1(c) shows the layout with magnets. Within the gap there is a pair of quadrupoles separated by a distance sL_0, and the distance between each of the magnets to the corresponding end of the tube is given by aL_0. So $2a + s = 1$. With magnets, the matrix M_{gap} is to take on the following form:

$$M_{gap} \to S(aL_0)M(f)S(sL_0)M(-f)S(aL_0)$$
$$= \begin{bmatrix} 1 + \frac{s}{b} - \frac{as}{b^2} & [1 - \frac{a^2s}{b^2}]L_0 \\ -\frac{s}{b^2L_0} & 1 - \frac{s}{b} - \frac{as}{b^2} \end{bmatrix}, \qquad (15)$$

where $b = f/L_0$ and f is the magnitude of the focal length which is assumed to be the same for both the convergent and the divergent quadrupoles. The magnet matrix in the thin lens approximation, for focal length f, is given by

$$M(f) = \begin{bmatrix} 1 & 0 \\ -\frac{1}{f} & 1 \end{bmatrix}. \qquad (16)$$

Collider Physics VIII

Minimization strategy of emittance growth due to LWFA betatron effects

$$\epsilon \propto \langle \Omega^3 \rangle \propto (\sin\psi_m)^{3/2},$$

a. Super Unit with chips

b. Accelerator Layout

the local wakefield, as defined earlier, is ψ_s, then the electron phase relative to the laser pulse defined by the local plasma wave number k_p is

$$k_p s_1 = 2\pi N_{\rm load} - \psi_s,$$

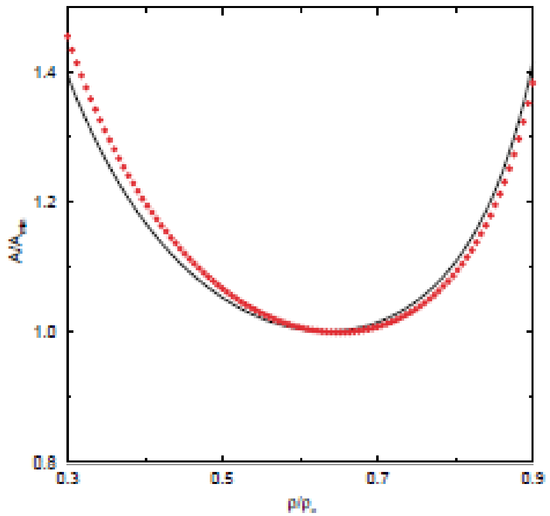

FIG. 8. (Color) Relationship between the normalized cross section and the normalized density function in a nozzle flow. The solid circles are for the monoatomic plasma and the curve is for the diatomic plasma.

$$\frac{1}{k_p}\frac{dk_p}{dz} = \frac{1}{2\pi N_{\rm load} - \psi_s}\frac{d\psi}{dz} = \frac{1}{2(2\pi N_{\rm load} - \psi_s)c}\frac{\omega_p^3}{\omega_0^2}. \quad (35)$$

a. Horn Model

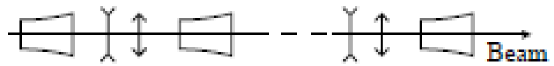

b. Synchronous Condition

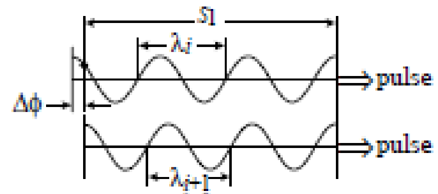

$$s_1 = \frac{2\pi N_{\rm load} - \Delta\phi}{k_i} = \frac{2\pi N_{\rm load}}{k_{i+1}}$$

FIG. 9. The horn model. (a) Matching condition for synchronous acceleration for the case where $\psi_s = 0$. (b) A schematic layout of the horn model.

$$\Delta\epsilon = \epsilon_f - \epsilon_0 \propto \frac{(\sin\psi_m)^{3/2}\sigma_D^2}{N}.$$

Chiu et al (2000)

Etat de l'Art
HEEAUP 2005

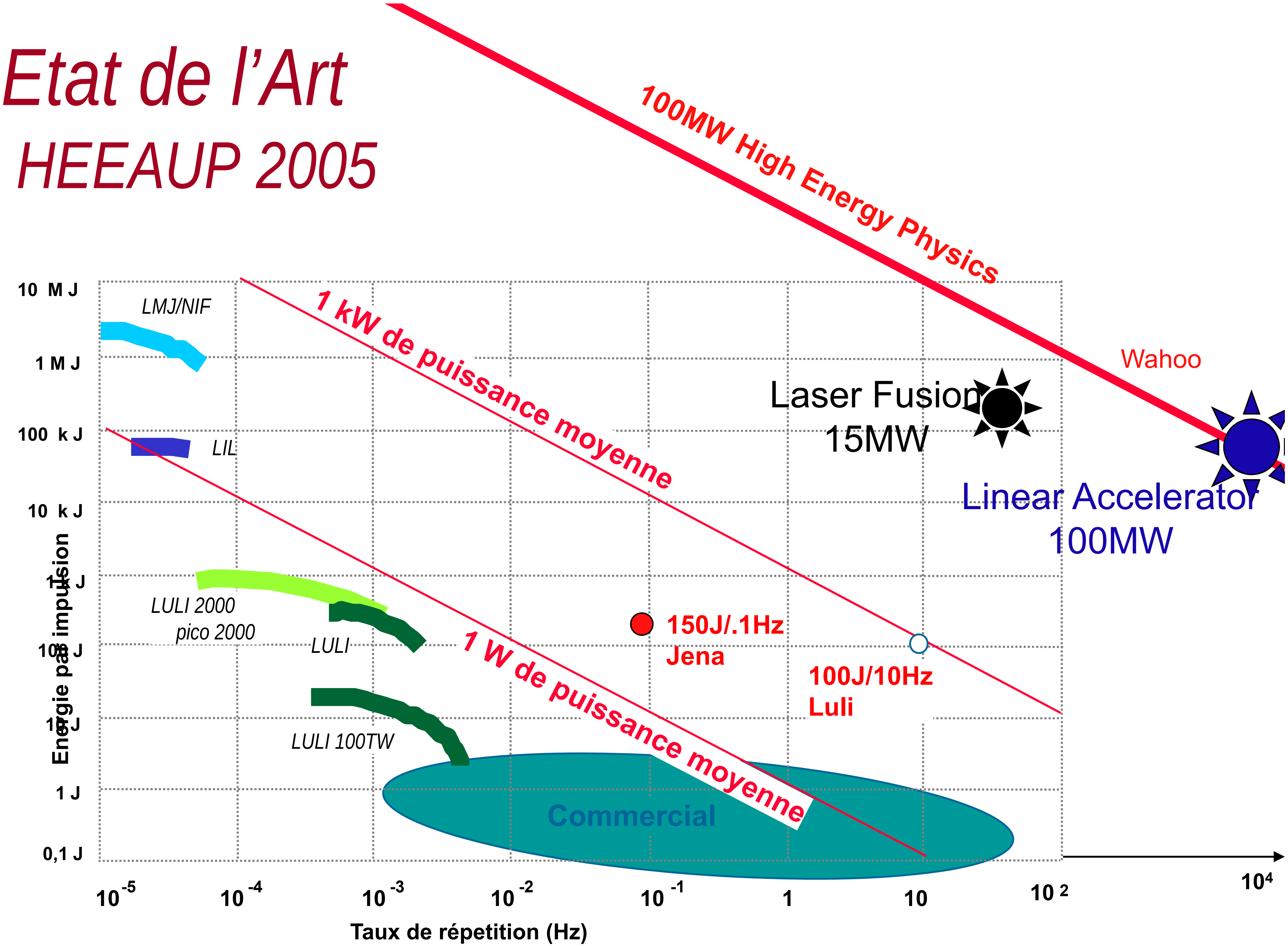

G. Mourou (2005)

The bottleneck in high-power lasers is the average power !

„Beyond Petawatt means Kilowatt“

W. Sandner (2010)

Proposal to form a consortium to study high efficiency, high rep rate fiber laser system:

ICAN, International Coherent Amplification Network

"Solving the efficiency problem in high peak and high average power laser: an international effort"

(Coordinator G. Mourou, submitted to the EU November 25, 2010)

Now in a shortlist in EU (March, 2011)

Fiber vs. Bulk lasers

- High Gain fiber amplifiers allow ~ 40% total plug-to-optical output efficiency
- Single mode fiber amplifier have reached multi-kW optical power.
- large bandwidth (100fs)
- immune against thermo-optical problems
- excellent beam quality
- efficient, diode-pumped operation
- high single pass gain
- They can be mass-produced at low cost.

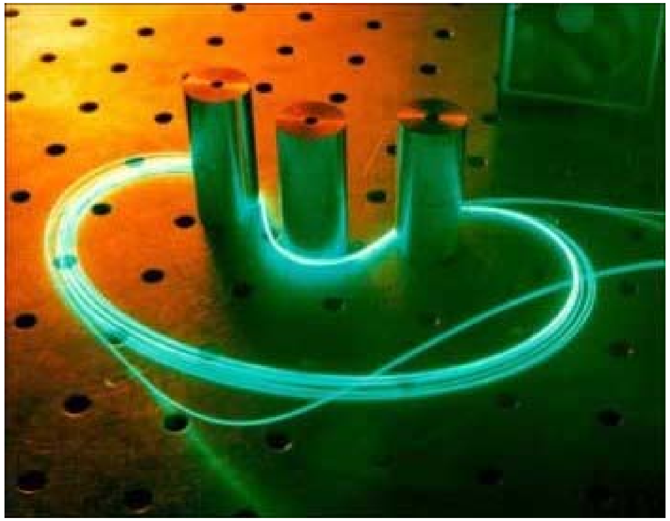

(G. Mourou)

CAN (Coherent Amplifying Network) Group

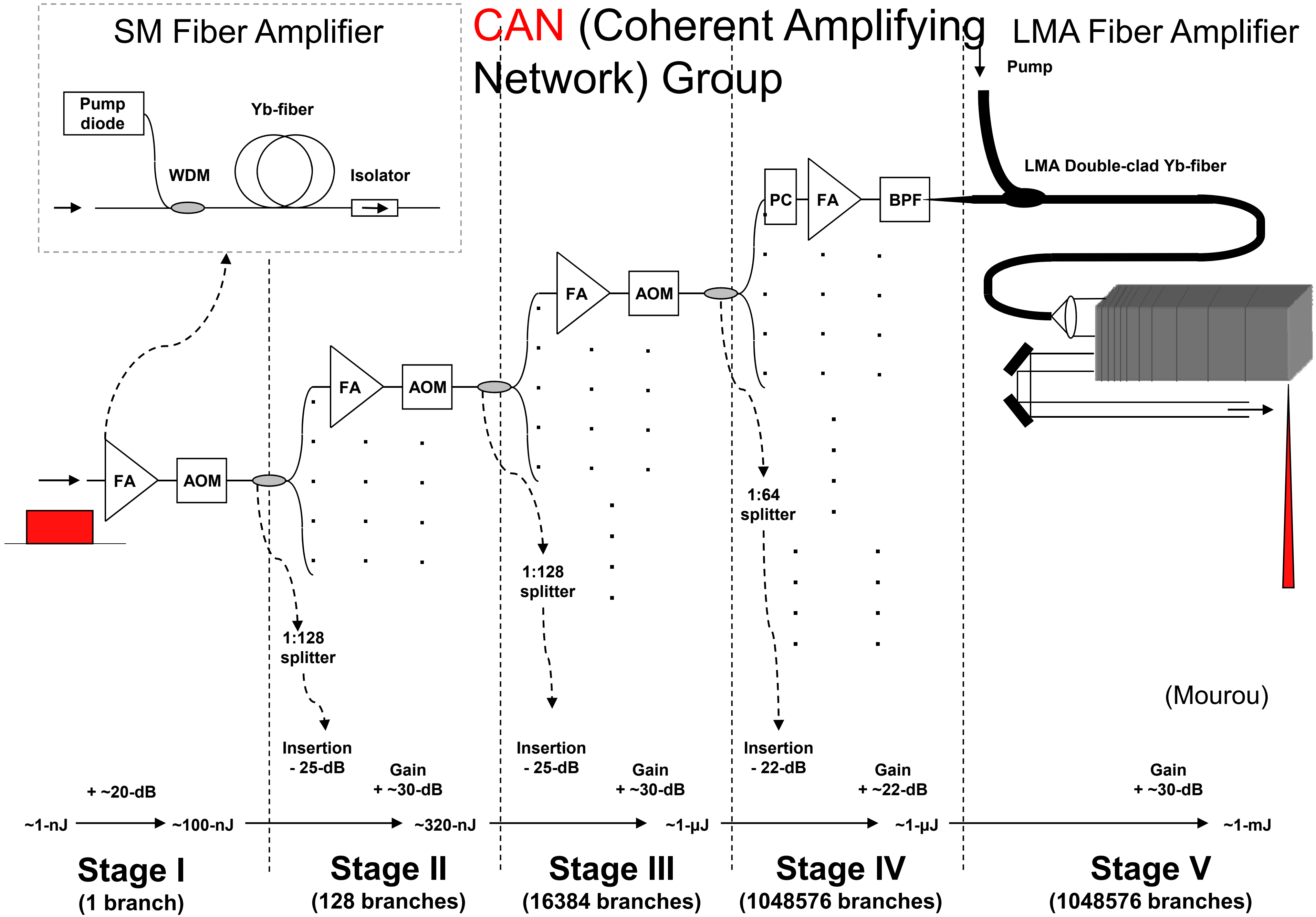

(Mourou)

1.5 MW Fiber bundles (x100)

Because the transport fibers are lossless they will be assembled
in a bundle just before the focusing optics. They will be
all coherently phased.

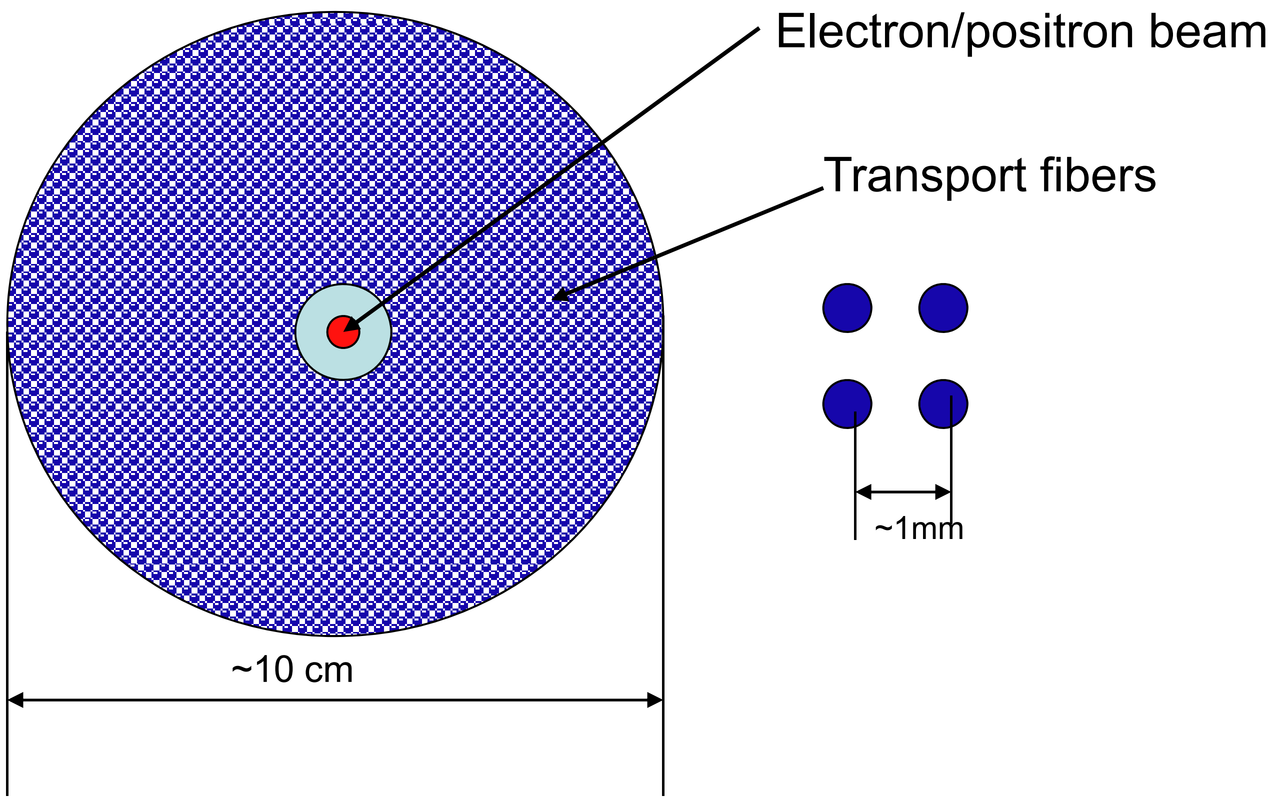

Length of a fiber ~5m   Total fiber length~ $5\ 10^4$km

(Mourou et al)

Nuclear Wake?

- BNL (and CERN) heavy ion collider: **"monojet"**
- Could be caused by:
  - Large angle gluon radiation (Vitev and Polsa and Salgado).
  - Deflected jets, due to flow (Armesto, Salgado and Wiedemann) and/or path length dependent energy loss (Chiu and Hwa).
  - Hydrodynamic conical flow from mach cone shock-waves (Stoecker, Casalderrey-Solanda, Shuryak and Teaney, Renk, Ruppert and Muller).
  - Cerenkov gluon radiation (Dremin, Koch).
- Jet quenching: collective deceleration by wakefield?
  - LWFA method, or Maldacena method?

PHENIX PRL 97, 052301 (2006) | Horner (STAR) QM2006

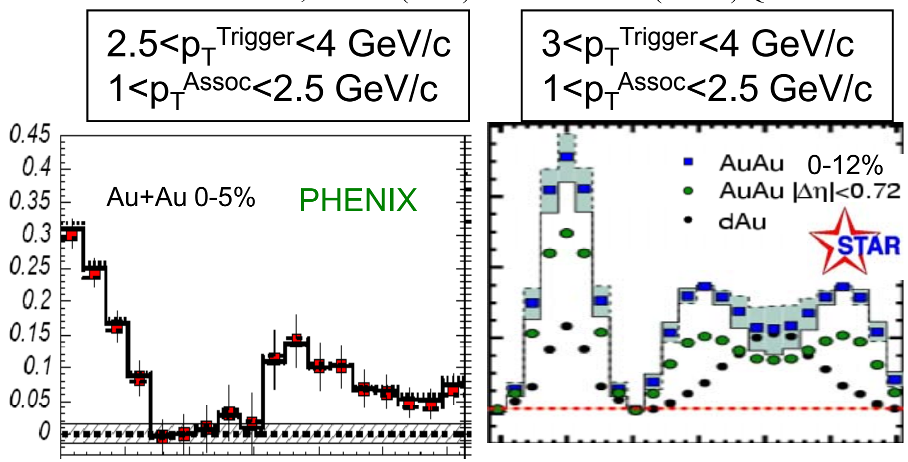

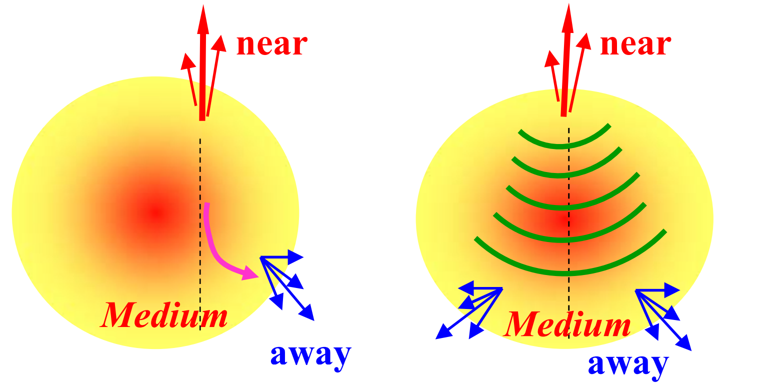

Deflected Jets | Conical Emission

Wakefield even inside of a nucleus

All particles in the medium participate = collective phenomenon

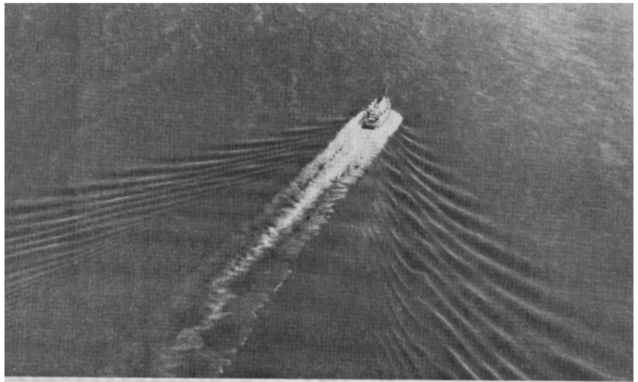

Рис. 71. Наблюдаемая картина корабельных волн. [Любезно предоставлено Aerofilms Ltd.]

Kelvin wake

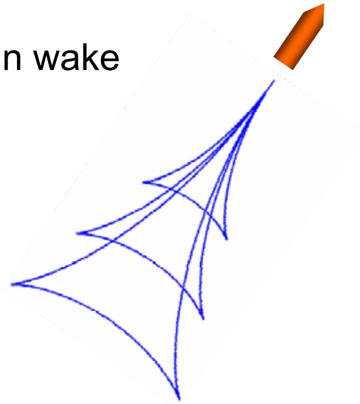

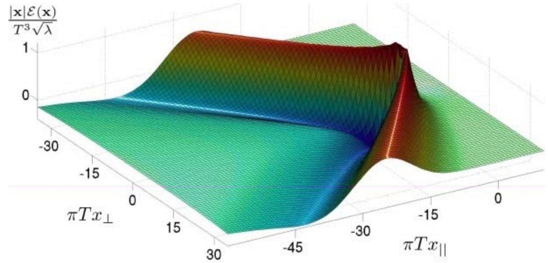

Maldacena method: QCD **wake**
(Chesler/Yaffe 2008)

No wave breaks and wake **peaks** at v≈c

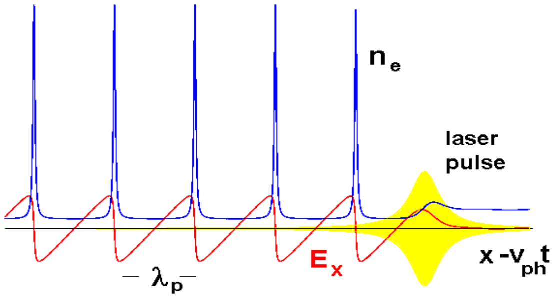

← relativity regularizes

Wave **breaks** at v<c

(The density cusps.
Cusp singularity)

(Plasma physics vs.
String theory?)

Challenge Posed by DG Suzuki

Frontier science driven by advanced accelerator

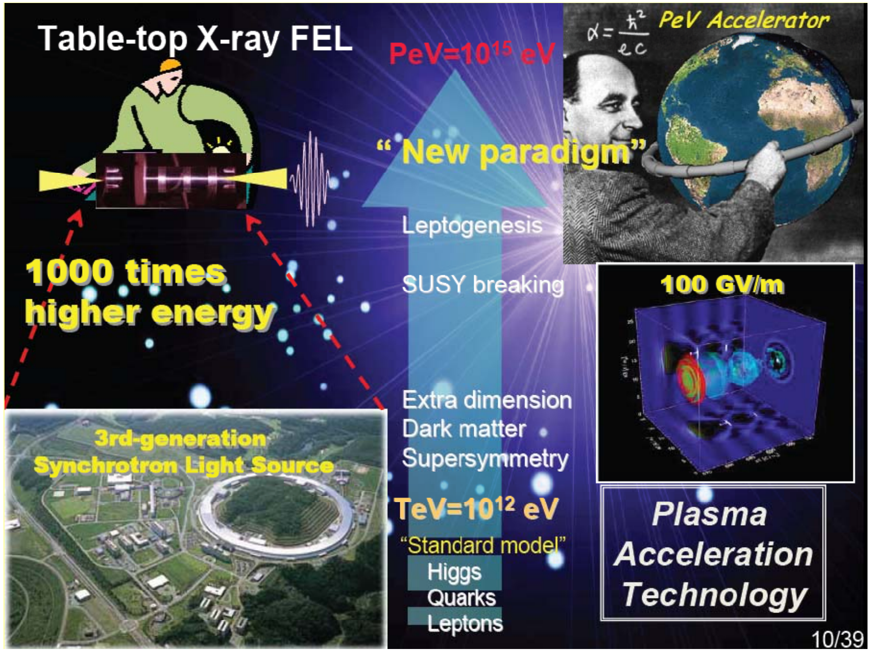

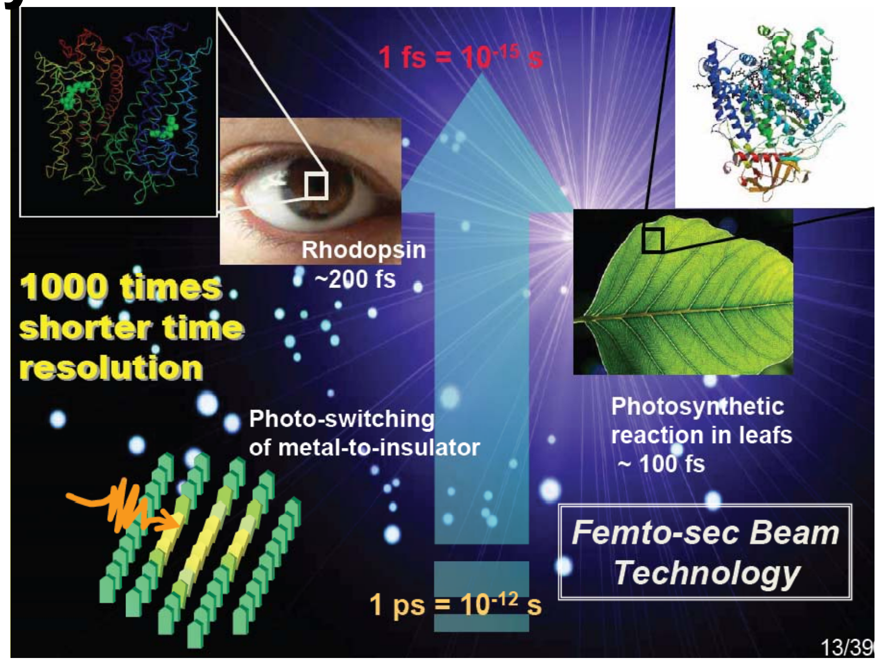

compact, ultrastrong *a*

atto-, zeptosecond

Can we meet the challenge?

A. Suzuki @KEK(2008)

Theory of wakefield toward extreme energy

$$\Delta E \approx 2m_0c^2a_0^2\gamma_{ph}{}^2 = 2m_0c^2a_0^2\left(\frac{n_{cr}}{n_e}\right),$$ (when 1D theory applies)

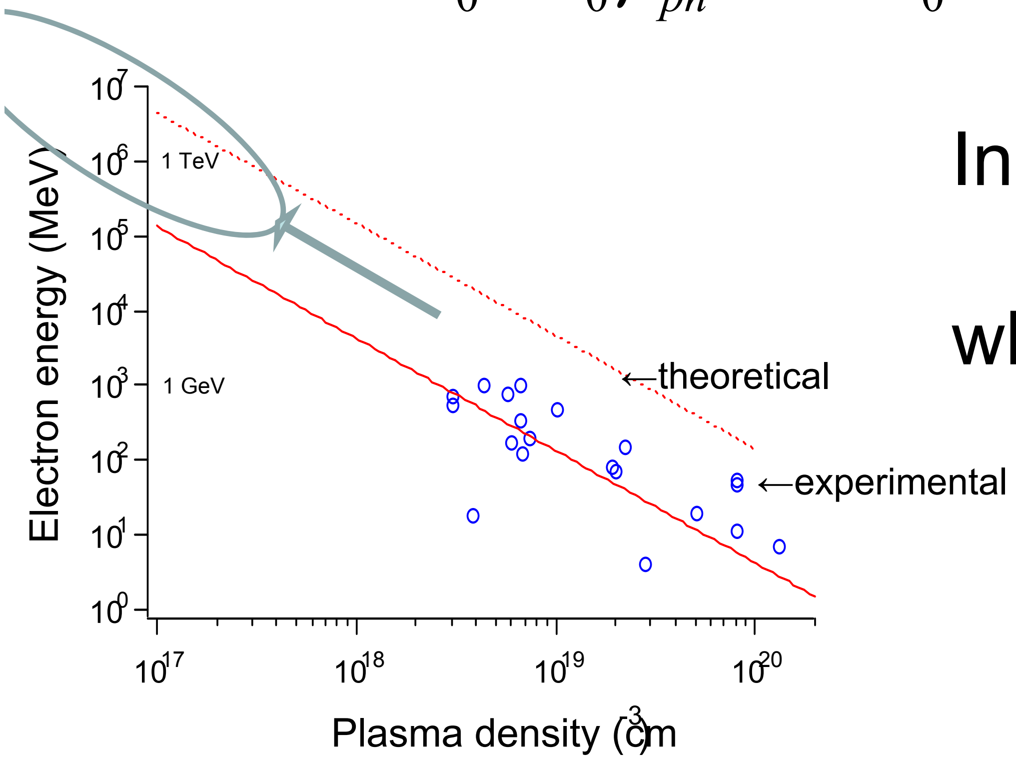

In order to avoid wavebreak,

$$a_0 < \gamma_{ph}{}^{1/2},$$

where

$$\gamma_{ph} = (n_{cr} / n_e)^{1/2}$$

$$L_d = \frac{2}{\pi}\lambda_p a_0^2\left(\frac{n_{cr}}{n_e}\right),$$

dephasing length

$$L_p = \frac{1}{3\pi}\lambda_p a_0\left(\frac{n_{cr}}{n_e}\right),$$

pump depletion length

Adopt:

NIF laser (3MJ)

→ 0.7PeV

(with Kando, Teshima)

Wakefield Acceleration for Compact EHECR

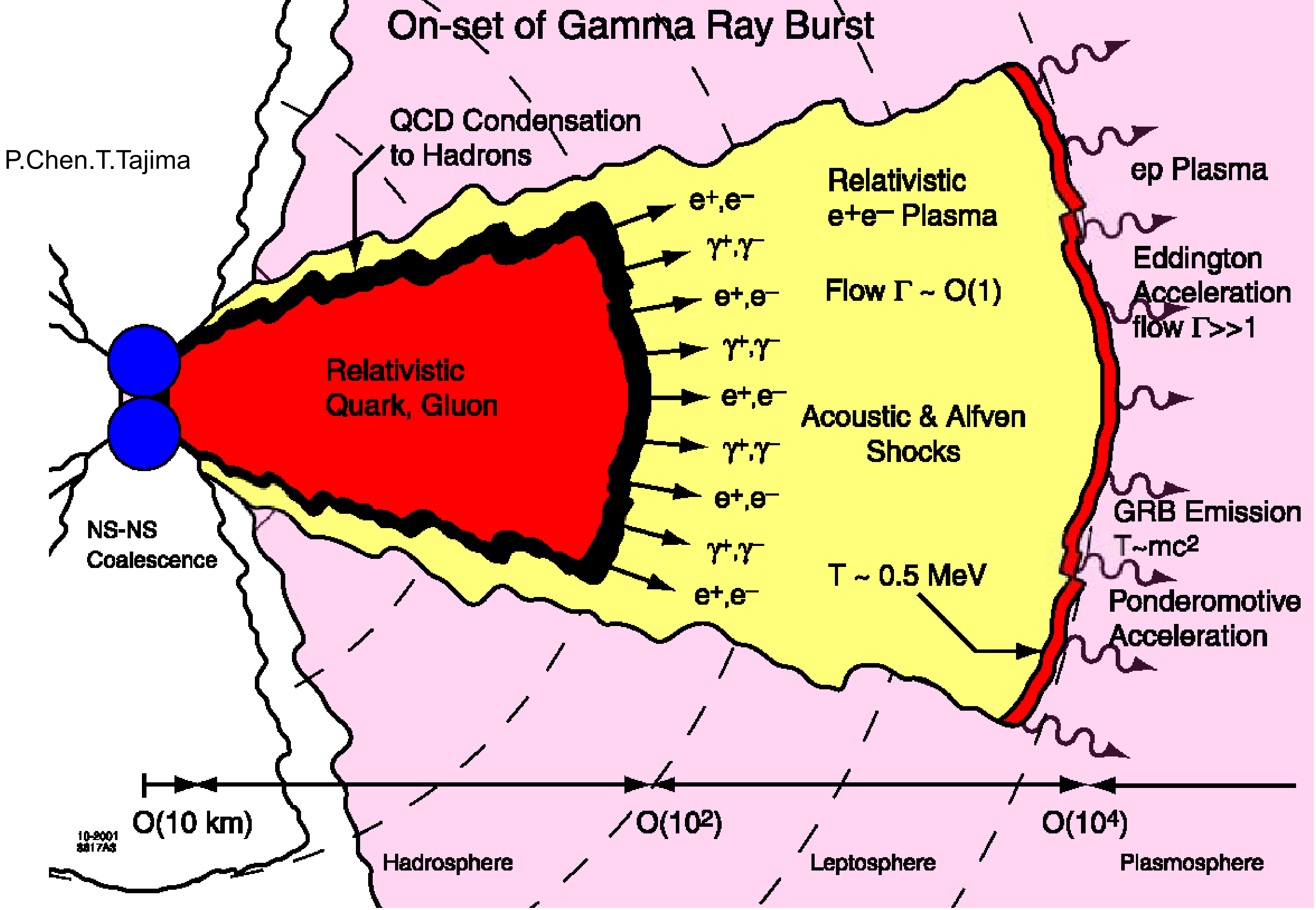

γ-ray signal from primordial GRB

LETTERS NATURE

(Abdo, et al, 2009)

←lower energy

higher→

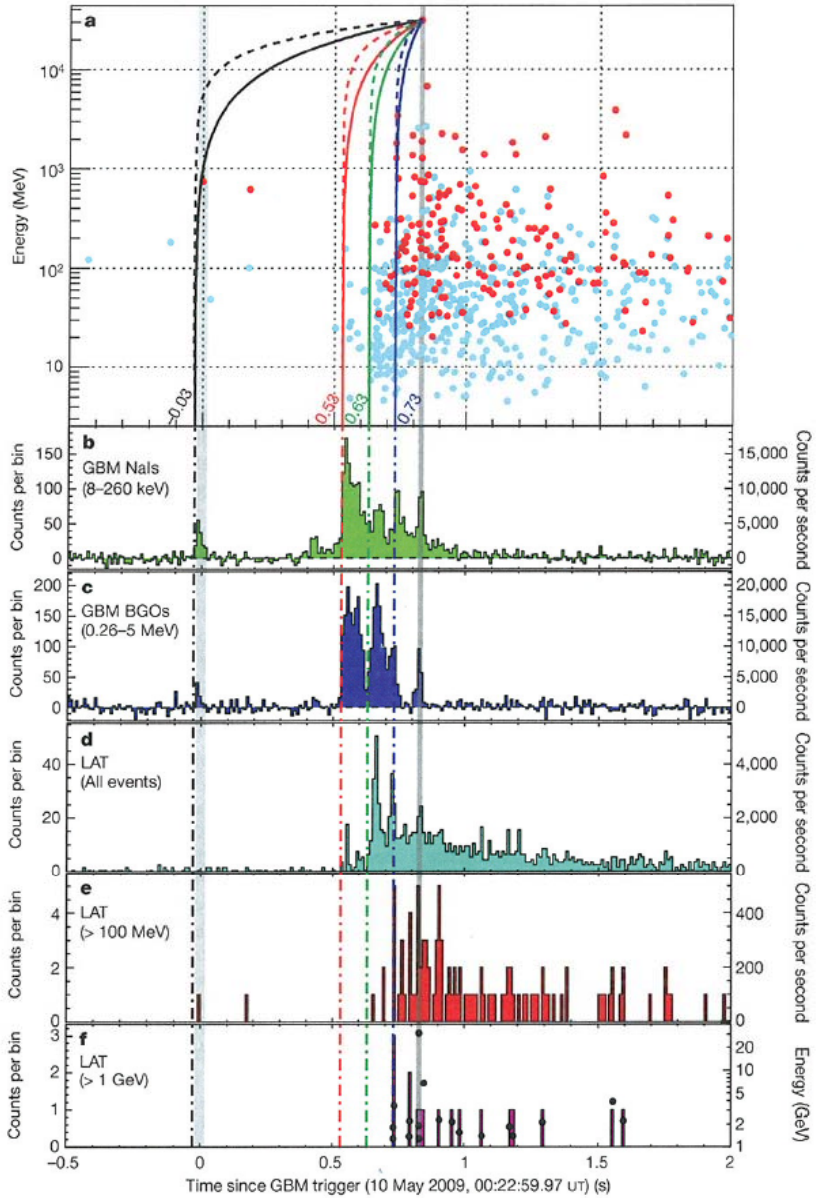

Figure 1 | Light curves of GRB 090510 at different energies. a, Energy lowest to highest energies. **f** also overlays energy versus arrival time for each

Energy-dependent
photon speed ?
Observation of primordial
<u>Gamma Ray Bursts (GRB)</u>
(limit is pushed up close to Planck mass)

Lab PeV γ (from e-) can explore this with control

Feel vacuum texture: PeV energy γ

Laser acceleration → controlled laboratory test to see quantum gravity texture
on photon propagation (Special Theory of Relativity: c_0)

$c < c_0$

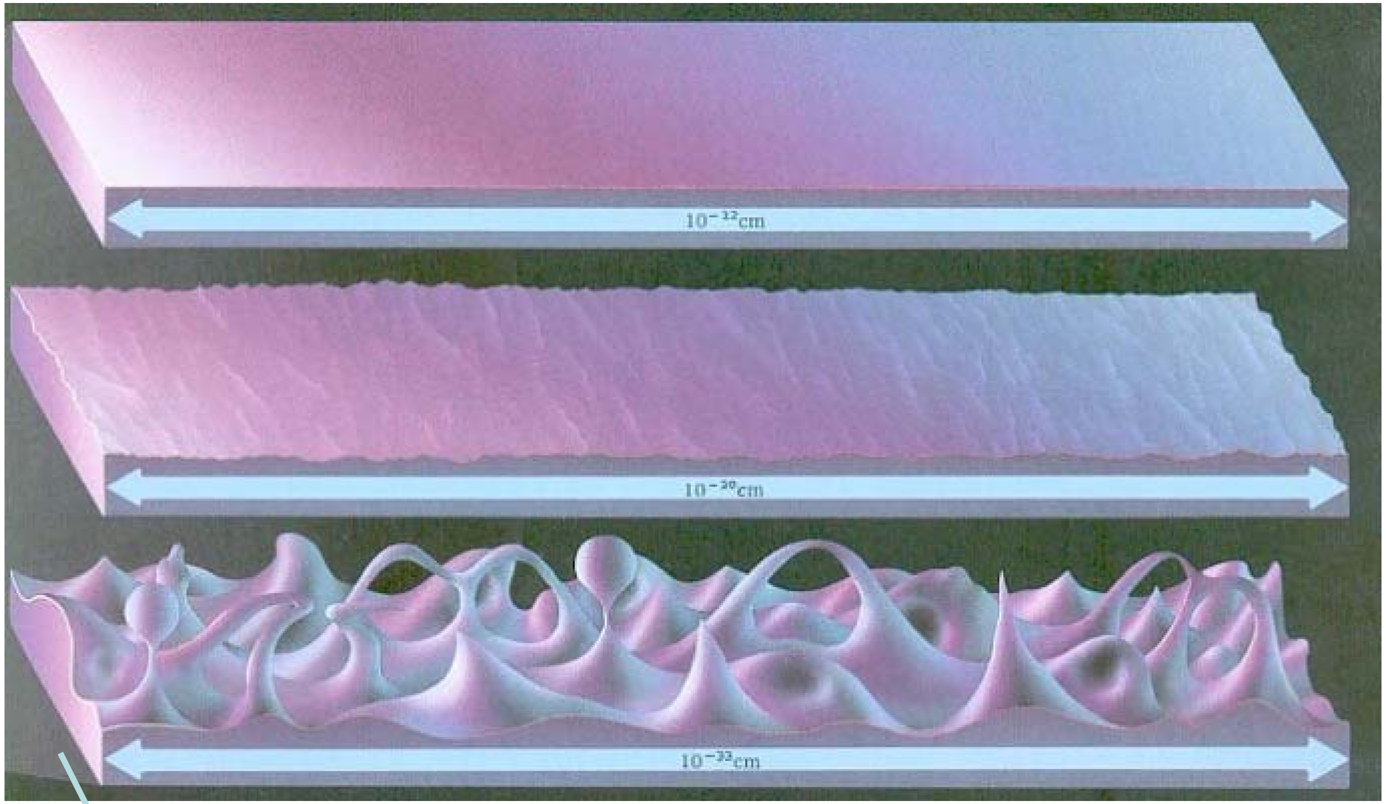

Coarser, lower energy texture

Finer, higher energy texture

← (0.1PeV)

1km ←(1PeV : fs behind)

PeV γ (converted from e^-)

Attosecond Metrology of PeV γ Arrivals

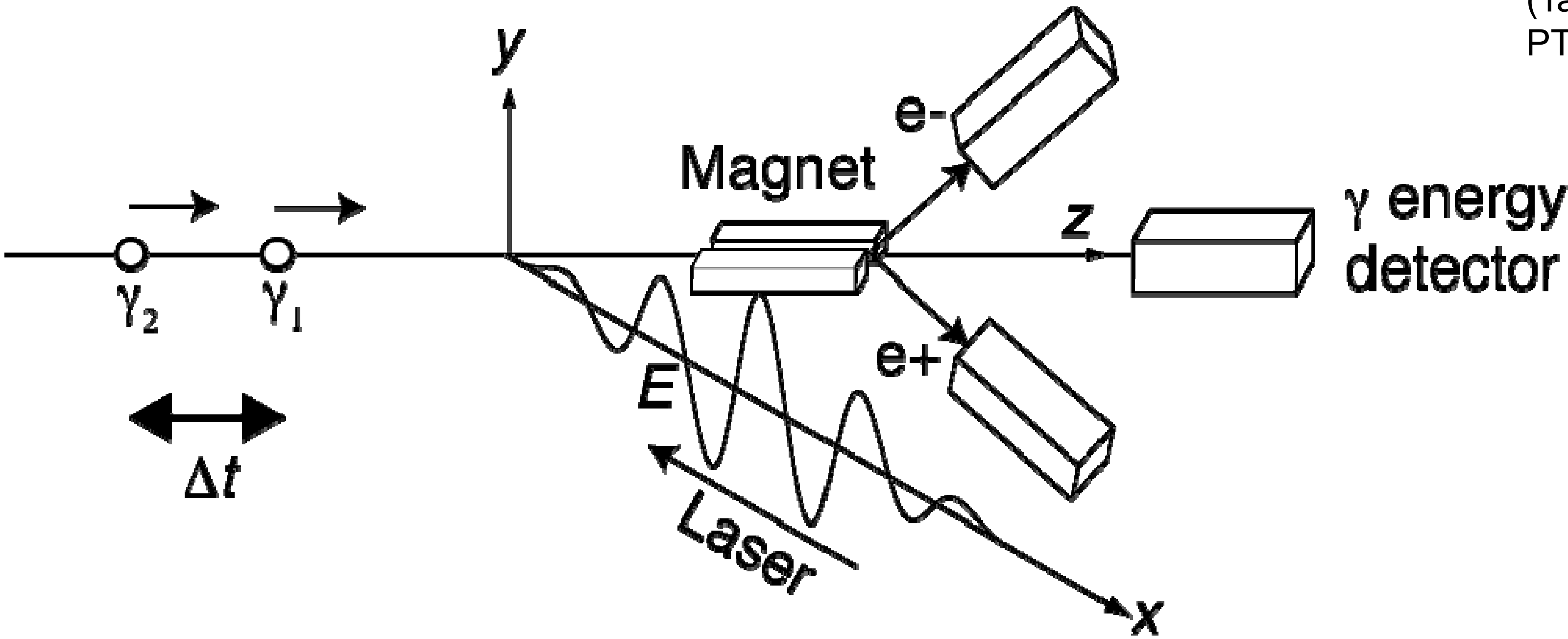

(Tajima, Kando, PTP, 2011)

High energy γ- induced Schwinger breakdown (Narozhny, 1968)
CEP phase sensitive electron-positron acceleration
Attosecond electron streaking
γ- energy tagging possible

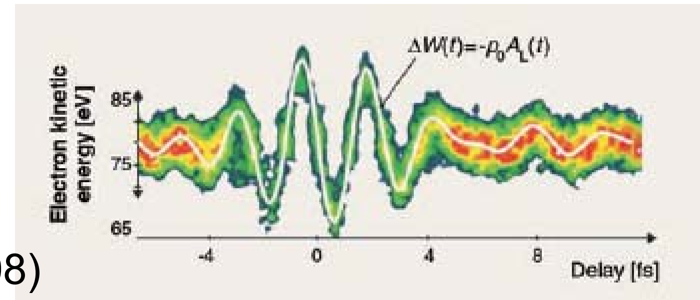

Goulielmakis(2008)

Domains of physical laws materialized

We may be simply driven by our ability to see !

Cosmological observation

Weak coupling
m=0

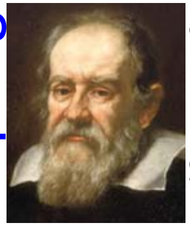

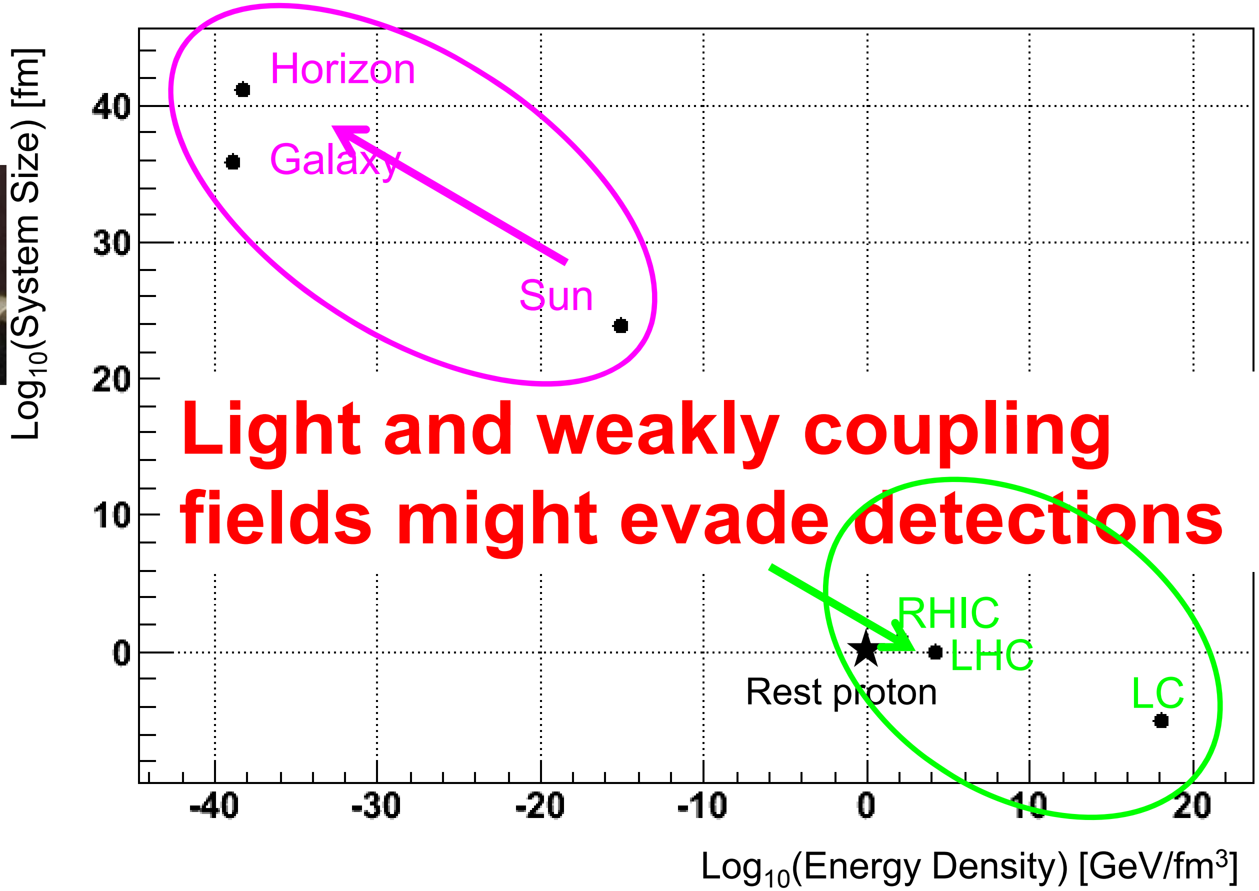

Light and weakly coupling fields might evade detections

Strong coupling
Heavy m

High energy collider

Homma, Habs, Tajima: to be published

Accessible subjects by high-intensity lasers

① Laser-laser interactions: new particle search in vacuum

Laser-induced non-linear effect in vacuum ← Non-linear effect in crystal

Birefringence

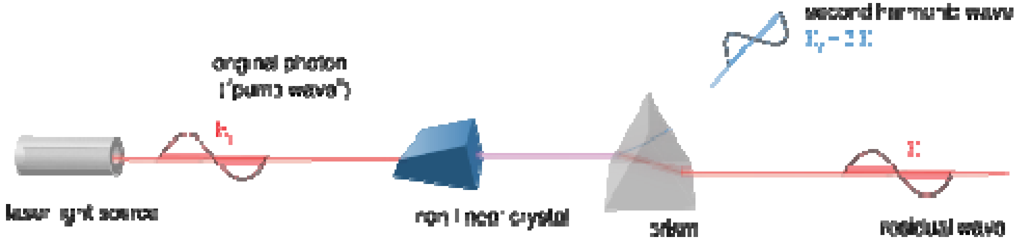

Second harmonic generation

Higher harmonic generation

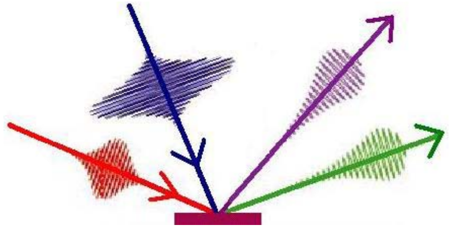

② Laser-γ interactions: non-perturbative aspect of vacuum

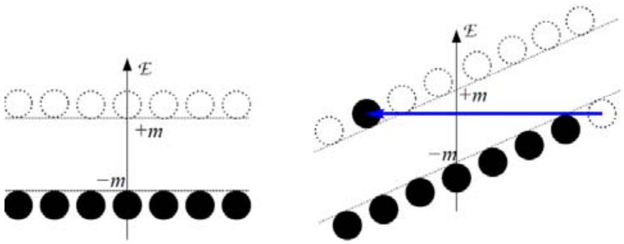

QED tunneling

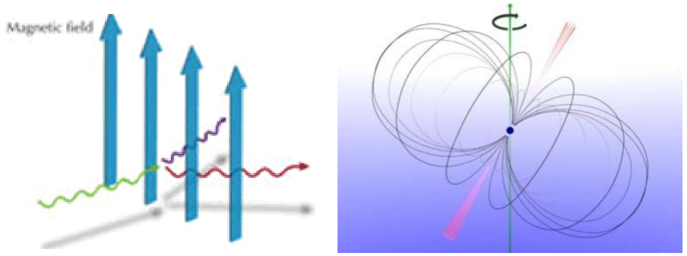

Photon splitting (magnetor)

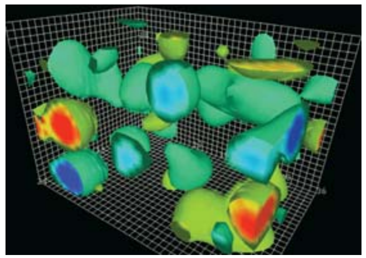

QCD vacuum

(Homma)

Birefringence by QED in eV range

Euler-Heisenberug effective one loop action

$$L_{QED} = \frac{1}{360}\frac{\alpha^2}{m^4}[4(F_{\mu\nu}F^{\mu\nu})^2 + 7(F_{\mu\nu}\widetilde{F}^{\mu\nu})^2]$$

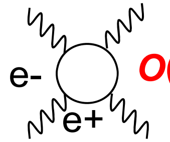

O(10^-42^b)

Refractive index depends on polarization relation

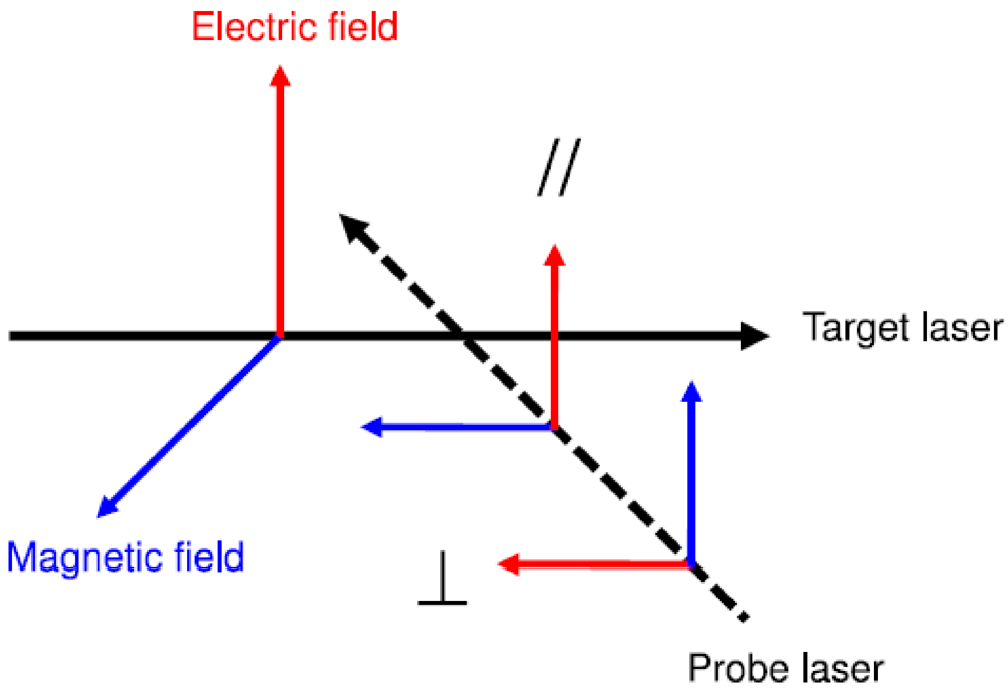

$$n_{\parallel} = 1 + \frac{16}{45}\frac{\alpha^2 U}{U_e}, \quad n_{\perp} = 1 + \frac{28}{45}\frac{\alpha^2 U}{U_e}$$

$U_e = m_e^4 c^5/\hbar^3 \approx$ 1.42x10^6 J/μm^3

ELI(~200J per ~20fs) can reach $\Delta n \sim 10^{-9} \sim 10^{-10}$

Phase contrast imaging of vacuum

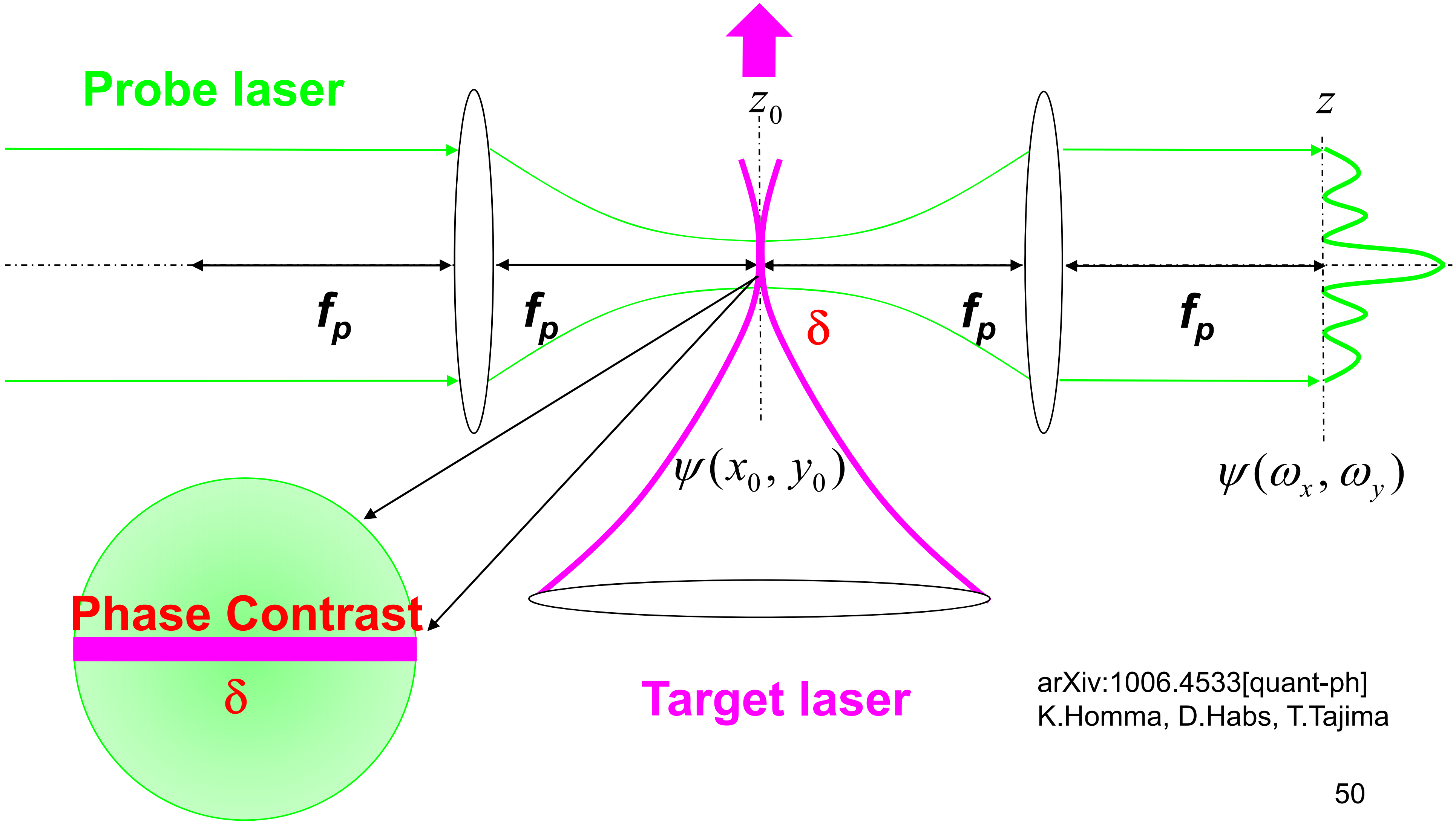

arXiv:1006.4533[quant-ph]
K.Homma, D.Habs, T.Tajima

Beyond photon-photon interaction in QED

$$L_{QED} = \frac{1}{360}\frac{\alpha^2}{m^4}[4(F_{\mu\nu}F^{\mu\nu})^2 + 7(F_{\mu\nu}\tilde{F}^{\mu\nu})^2]$$

$$\phi F_{\mu\nu}F^{\mu\nu} \qquad \sigma F_{\mu\nu}\tilde{F}^{\mu\nu}$$

QCD and low-mass scalar ϕ and pseudoscalar σ may change 4 : 7

Resonance in quasi-parallel collisions in low cms energy

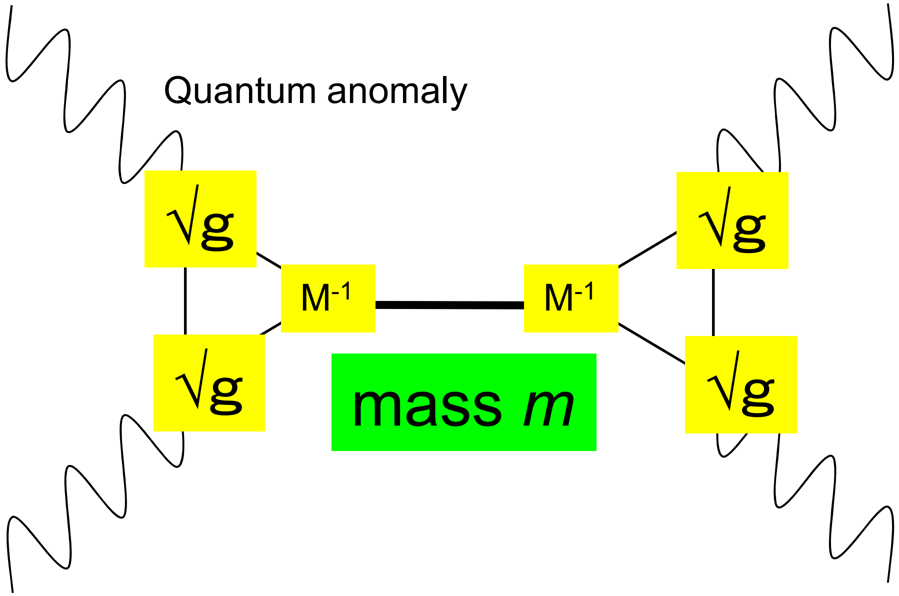

If M~M$_{Planck}$, Dark Energy

$$gM^{-1}F^{\mu\nu}F_{\mu\nu}\phi$$

arXiv:1006.1762 [gr-qc]
Y. Fujii and K.Homma

QCD-instanton, Dark Matter

$$gM^{-1}F^{\mu\nu}\tilde{F}_{\mu\nu}\sigma$$

arXiv:1103.1748 [hep-ph]
K.Homma, D.Habs, T.Tajima
Accepted

Resonance production of light field
- how to reduce center of mass energy -

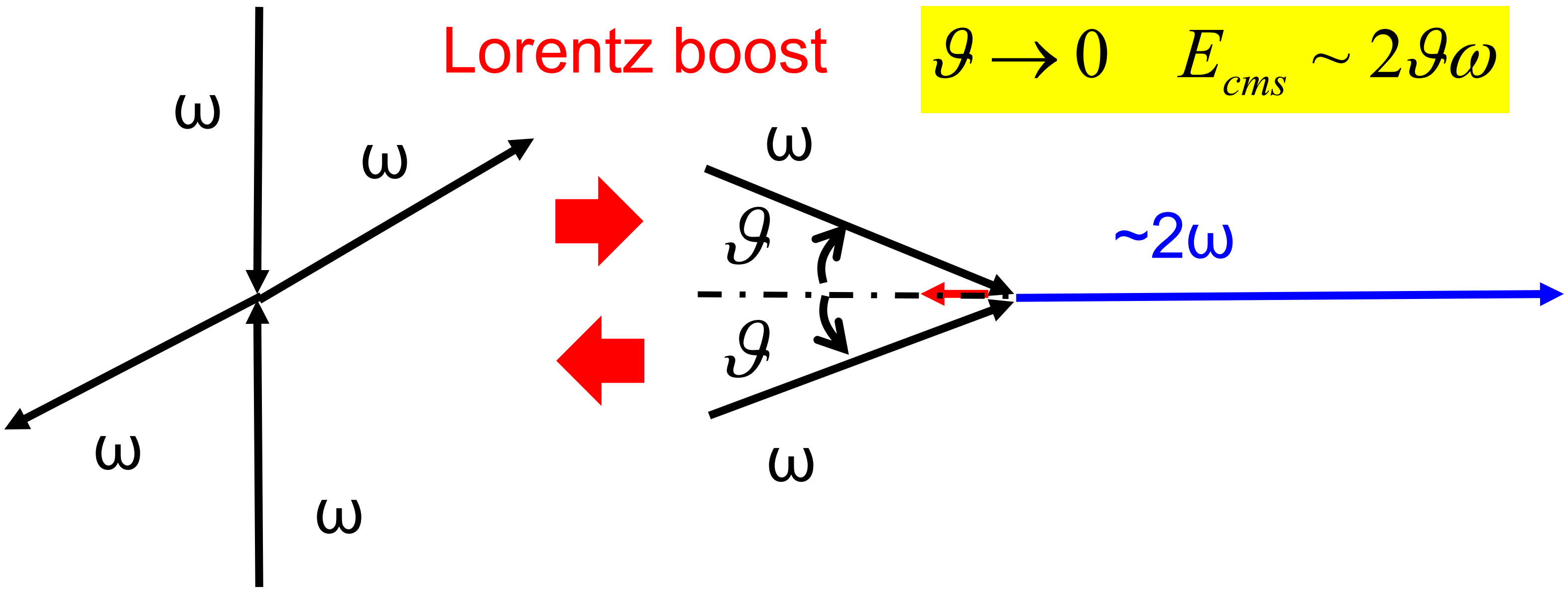

Center of Mass System

Quasi Parallel System

No frequency shift

- **Frequency shift on the boost axis**
- **Lower Ecms by *θ* keeping ω constant**

Low frequency photon in QPS is an ideal system !

Degenerated Four-Wave Mixing (DFWM)

Laser-induced non-linear effect in vacuum <= Non-linear effect in crystal

Decay into 3ω can be induced by frequency-mixing.

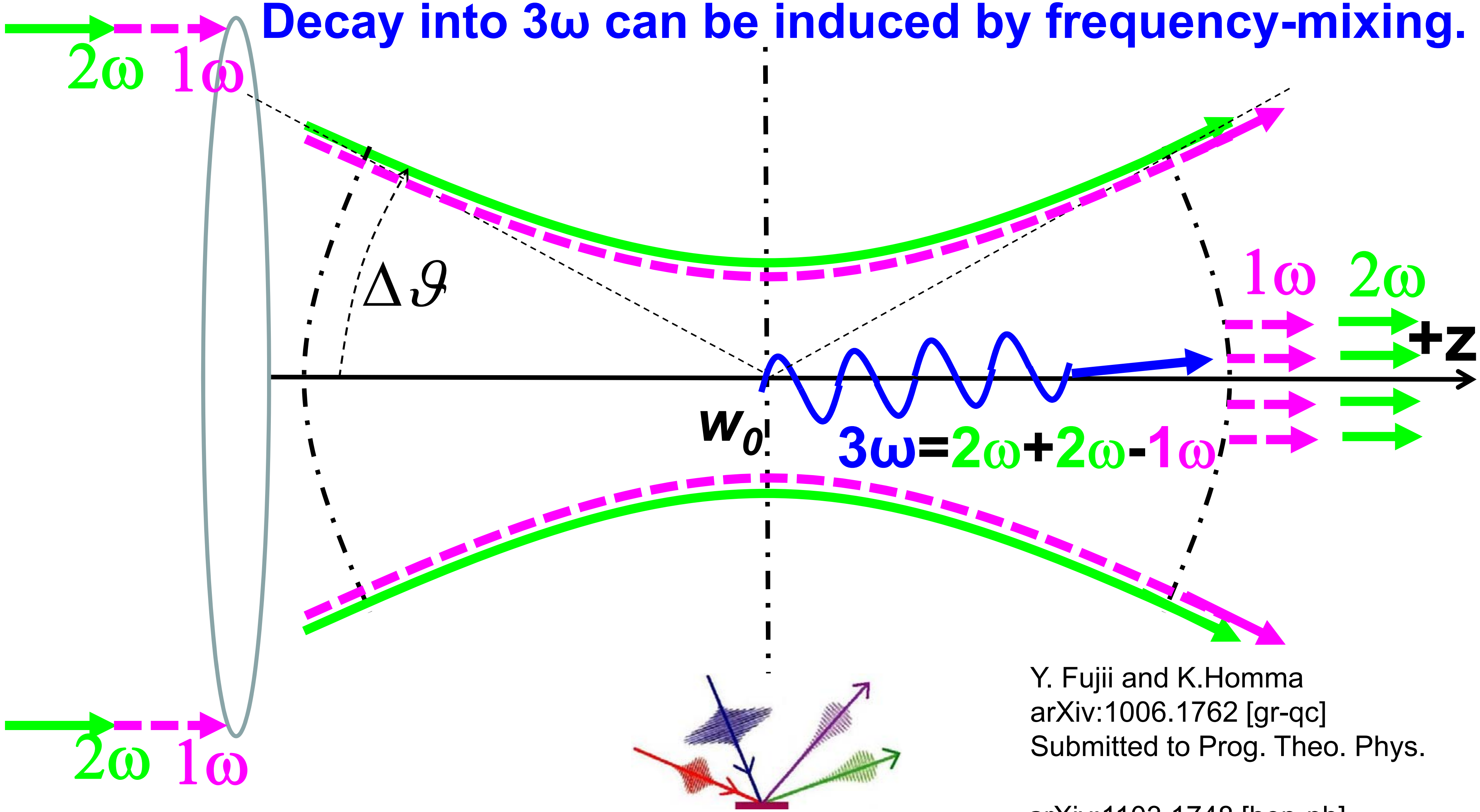

Y. Fujii and K.Homma
arXiv:1006.1762 [gr-qc]
Submitted to Prog. Theo. Phys.

arXiv:1103.1748 [hep-ph]
K.Homma, D.Habs, T.Tajima
Accepted by Appl. Phys. B

HFS road to unknown fields: dark matter and dark energy

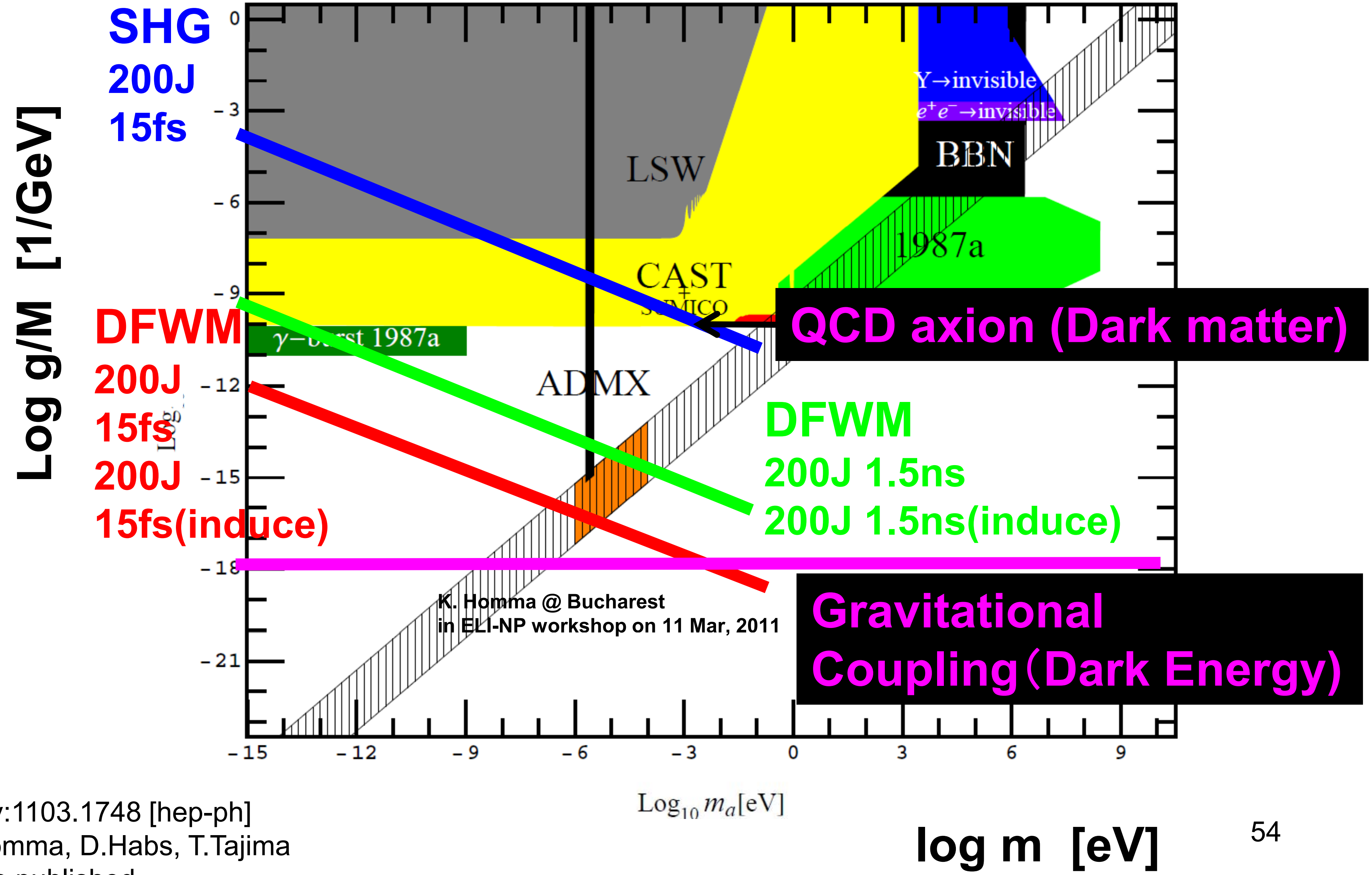

arXiv:1103.1748 [hep-ph]
K.Homma, D.Habs, T.Tajima
To be published

conclusions

- LWFA provides unique and new tool for a variety of applications
- Bridge between accelerator and laser communities necessary-----a Bridgelab, ICUIL-ICFA collaboration
- Collider physics requirements: luminosity maximization, small beam, large betatron, emittance preservation: tough challenges
- Driver laser for collider: a huge challenge, but possible technologies emerging
- Energy frontier with precision w/ a few shots possible
- High field science approach: capability to explore undiscovered new fields

Centaurus A:

cosmic
wakefield
linac?

Danke Schoen!